Université de Lomé

Universität Rostock

DRP-CCDRM

INTERNATIONAL MASTER PROGRAMME IN RENEWABLE ENERGY AND GREEN HYDROGEN

SPECIALITY: Bioenergy/Biofuels and Green Hydrogen Technology

MASTER THESIS

Subject/Topic:

INVESTIGATION OF HYDROGEN PRODUCTION BY DARK CO-FERMENTATION OF WATER HYACINTH AND BANANA PEELS

2021-2023

Presented on the 26th September 2023

by:

Djangbadjoa GBIETE

Exam Committee members :

Chair : Amivi TETE-BENISSAN, Professor, Université de Lomé - Togo

Examiner/judge : Koffigan AGBATI, Associate Professor, Université de Lomé - Togo

Main Supervisor: Damgou MANI KONGNINE, Associate Professor, Université de Lomé - Togo

Co-Supervisor: Satyanarayana NARRA, Professor, University of Rostock - Germany

WASCAL West African Science Service Centre on Climate Change and Adapted Land Use

Federal Ministry of Education and Research

DECLARATION

I hereby declare that I have written this master's thesis titled "Investigation of Hydrogen Production by Dark Co-Fermentation of Water Hyacinth and Banana Peels" by myself, using permitted reference sources and materials. All the references and materials that I have used are appropriately cited. Additionally, I declare that this thesis has not been submitted to any other academic examination anywhere else.

Rostock, 14th August 2023 Djangbadjoa GBIETE

DEDICATION

I dedicate this thesis work to my parents and my brothers and sisters for their unwavering support throughout my academic cursus. The greatest honor is to my lovely mother Tchandame SAMBIANI, and my brothers Nampouguini KPANKPANE and Damename GBIETE for everything they've done for me in my life.

I also dedicate this thesis to my godfather Prof. Minlipe Martin GANGUE, for his regular support and availability throughout my academic cursus.

ACKNOWLEDGEMENTS

First and foremost, I am highly thankful to the German Federal Ministry of Education and Research (BMBF) and the West African Science Service Center on Climate Change and Adapted Land Use (WASCAL) for granting me the scholarship without which I would not have achieved this academic journey. I hereby express my appreciation for pursuing my studies under this scholarship.

I Would like to express my gratitude to Université Abdou Moumouni, Université de Lomé, and Universität Rostock. My first and second semesters were done at Université Abdou Moumouni, Niger, my third semester at Université de Lomé, Togo while the fourth semester for internship and thesis writing was done at Universität Rostock, Germany.

I am very much thankful to my Advisor Dr. Damgou MANI KONGNINE, also the Scientific Coordinator of this Master's speciality, for his involvement and support throughout. I would like to offer him my sincere gratitude for his constant technical support, academic guidance, and pertinent feedback throughout my work. His patience and immense experience noticeably contributed to the impact of this work. I deeply appreciated the opportunity to work under Dr. Mani's supervision.

I extend my gratitude to Prof. Dr. habil. Satyanarayana Narra, my co-Supervisor and also the General Coordinator of this Master's Speciality at Universität Rostock, Germany, for his noticeable support, guidance, and availability throughout my study. His pertinent feedback, comments, and motivation helped me achieve this work. I always appreciate the opportunity to work under Prof. Narra's guidance.

I would like to equally express my sincere thanks to my second Co-Supervisor Dr-Ing. Jan Sprafke, for his outstanding technical support, guidance, and feedback throughout my thesis internship. His immense laboratory experience and knowledge, and his availability helped me achieve this work. I was only able to perform my laboratory experiments thanks to his invaluable support. I hereby express my deepest appreciation for the opportunity to work with Dr.-Ing. Jan.

I extend my sincere gratefulness and appreciation to Dr. Komi AGBOKA, the Director of WASCAL GSP at Université de Lomé, for his remarkable support and availability throughout this Master.

My gratitude does not overlook the support and motivation I received from Prof. Rabani ADAMOU, the Director of WASCAL GSP at Université Abdou Moumouni during the first year of my Master.

I am highly thankful to Dr. Komi BEGEDOU, the Deputy Director of WASCAL GSP at Université de Lomé, for his constant support.

My sincere thanks go to Dr. Mouhamed IDRISSOU, the Scientific Coordinator of the WASCAL GSP at Université de Lomé, for his involvement and support.

I am very much grateful to Prof. Yendoubé LARE for his availability and guidance throughout my study. His advice and constant encouragement were invaluably helpful to me.

I would like to express my sincere thanks to Dr. Pali KPELOU and Dr. Essowè MOUZOU for their support and pertinent comments on this work.

Additionally, I could not end without thanking Kokou MALDJA and Dr. Fousseni FOLGA for their technical support.

Finally, but not the least, I would like to offer my sincere thanks to my colleagues, friends, and everyone who had contributed to this work in one way or another.

ABSTRACT

Climate change and fast-growing energy demand have triggered research for alternative sources of energy that are environmentally-friendly. Various clean energy sources have been extensively researched among which hydrogen as an energy carrier is found to be producible from biomass and waste resources. Water hyacinth, regarded as the worst aquatic plant due to its exponential invasiveness of aquatic environments, causes damage both to the environment and populations. In Lomé, water hyacinth invades lakes hindering economic and navigation activities. Its removal from the lakes generates heavy expenses and the harvested water hyacinth plants are landfilled. In an attempt to propose a sustainable solution to this situation, this study aimed to investigate hydrogen production by dark co-fermentation of water hyacinth and banana peels.

Water hyacinth leaves, stems, roots, and banana peels were dried and ground. The ground samples were characterized to determine their elemental composition, proximate analysis, and fiber content. The data from the characterization were used to simulate the dark co-fermentation process as well as the economic analysis of biohydrogen production by this process using SuperPro Designer®. Then, tests of biogas production from banana peels, water hyacinth leaves and stems were carried out.

Results showed that water hyacinth leaves, stems and banana peels had a suitable elemental composition for biohydrogen production. The volatile solid and cellulose contents of water hyacinth and banana peels revealed that these substrates had the necessary nutrients for biohydrogen production. The simulated co-fermentation produced 124,64, 110,52, 99,85, and 67,36 mL g^{-1} volatile solid for water hyacinth to banana peels mixing ratios of 100:0, 70:30, 50:50, and 0:100 respectively. The tests of biogas production from banana peels, water hyacinth stems, and leaves generated respectively 334.82, 324.79, and 280.15 mL g^{-1} volatile solid. It was therefore concluded that the production of hydrogen coupled with biogas generation and composting would be a promising option to valorize water hyacinth and banana peels wastes into energy in the city of Lomé.

Key words: water hyacinth; banana peels; dark fermentation; hydrogen; simulation.

RÉSUMÉ

Le changement climatique et la croissance rapide de la demande énergétique ont amplifié la recherche de sources d'énergies propres respectueuses de l'environnement. Diverses sources d'énergies propres ont fait l'objet de recherches scientifiques approfondies, parmi lesquelles l'hydrogène qui est un vecteur d'énergie, s'est révélé être productible à partir de la biomasse et des déchets organiques. La jacinthe d'eau, considérée comme la plante aquatique la plus nocive au regard de son expansion exponentielle en milieu aquatique, engendre des dégâts à la fois à l'environnement et aux populations. À Lomé, la jacinthe d'eau est présente dans la plupart des lacs, ce qui entrave les activités économiques et la navigation sur ces derniers. L'écurage des lacs envahis par la jacinthe d'eau engendre d'énormes dépenses économiques et une fois collectée, la jacinthe d'eau est déversée soit à l'air libre ou dans des fosses d'enfouissement. Afin de rendre cette activité plus efficiente, il est important de lui trouver une valeur ajoutée. Ainsi, cette étude a été conduite dans le but de valoriser la jacinthe d'eau en énergie, notamment pour la production du biohydrogène à partir de la co-fermentation sombre de la jacinthe d'eau et des pelures de bananes.

Les feuilles, les tiges, et les racines de jacinthe d'eau et les pelures de bananes ont été séchées et moulues. Les échantillons moulus ont été caractérisés afin de déterminer leurs compositions chimiques élémentaires ainsi que leurs teneurs en fibres. Les résultats de la caractérisation ont été utilisés pour simuler en utilisant le logiciel SuperPro Designer®, le processus de co-fermentation sombre ainsi que l'analyse économique de la production de biohydrogène à partir de ce processus. Ensuite, un test de production de biogaz à partir des échantillons moulus de feuilles et de tiges de jacinthe d'eau et de pelures de bananes a été effectué.

Les résultats ont montré que les feuilles et les tiges de jacinthe d'eau ainsi que les pelures de bananes ont une composition élémentaire appropriée pour la production de bio-hydrogène. La quantité des matières solides volatiles et celles cellulosiques de la jacinthe d'eau et des pelures de bananes ont révélé que ces dernières avaient les nutriments nécessaires pour la production de bio-hydrogène. La co-fermentation simulée a généré 124,64, 110,52, 99,85, et 67,36 mL g^{-1} de matières solides volatiles respectivement pour les ratios de mélange de 100:0, 70:30, 50:50, et 0:100 entre la jacinthe d'eau et les pelures de bananes. Le test de production de biogaz à partir des pelures de bananes, des tiges et des feuilles de jacinthe d'eau a généré respectivement 334,82, 324,79 et 280,15 mL g^{-1} de matières solides volatiles. Aussi, la

production d’hydrogène associée à la production du biogaz et du compost pourrait constituer une option intéressante de valorisation des déchets de jacinthe d’eau et de pelures de bananes en énergie dans la ville de Lomé.

Mots clés: jacinthe d’eau ; pelures de bananes ; fermentation sombre ; hydrogène ; simulation.

ACRONYMS AND ABBREVIATIONS

AC	Ash content
Acetyl-CoA	Acetyl-Coenzyme A
AD	Anaerobic digestion
ADF	Acid detergent fiber
ADL	Acid detergent lignin
ATP	Adenosine triphosphate
BMBF	German Federal Ministry of Education and Research
BP	Banana peels
CAPEX	Capital expenditure
F/M	Food to microorganism ratio
Fd	Ferrodoxin
FDH	Formate dehydrogenase
FHL	Formate hydrogen lyase
GHGs	Greenhouse gases
GSP	Graduate School Programme
HRT	Hydraulic retention time
IMP-EGH	International Master's Programme in Energy and Green Hydrogen Technology
LIBS	Laser-Induced Breakdown Spectroscopy
MC	Moisture content
MSW	Municipal solid waste
NADH	Nicotinamide adenine dinucleotide
NDF	Neutral detergent fiber
OPEX	Operation expenditure
OSW	Organic solid waste
PFOR	Pyruvate ferrodoxin oxidoreductase
SPD	SuperPro Designer®
SRT	Solid retention time
TS	Total solid

USD United States Dollars

VFAs Volatile fatty acids

VS Volatile solid

WASCAL West African Science Service Center on Climate Change and Adapted Land Use

WH Water hyacinth

WHL Water hyacinth leaves

WHR Water hyacinth roots

WHS Water hyacinth stems

wt% Weight percentage

LIST OF TABLES

LIST OF FIGURES

TABLE OF CONTENTS

INTRODUCTION

1. Background

Climate change has resulted in several environmental harms and societal impacts that are severely being coped with by living beings. The Rise in average temperature, the dramatic variations in rainfall, and the increase in extreme weather events are some of the manifestations of climate change. Human activities have caused the release of greenhouse gases into the atmosphere. Greenhouse gases trap heat above the earth's atmosphere and release it back to the earth. This has been the major driving force behind global warming. Human activity-related emissions are dominated by emissions from the energy sector, industries, forestry, land use, and land use change.

At the intersection of depleting fossil fuel reserves and exponential growth in energy demand, there is an urgent need to look for sustainable energy sources. Consequently, global decarbonization in the transportation, industry, and electricity generation sectors is required to mitigate human-caused climate change (Osman, Skillen, et al., 2020). In this regard, there has been a global growing interest in renewable energy sources as potential substitutes for fossil fuels. The development and deployment of renewable energy technologies are considered to be a backbone solution to the climate crisis as it significantly drives down carbon dioxide (CO_2) emissions. As reported by Aleixandre-Tudó et al. (2019), developing renewable energy technologies is key to addressing the world's two key challenges such as the mitigation of climate change and the necessity of rapidly meeting the increasing energy demand. Renewable energies such as solar, wind, biomass, geothermal, and hydroelectric power have the potential and are therefore critical to combat the energy crisis. Unlike fossil fuels, renewable energy preserves the environment, prevents environmental pollution, brings energy security, and triggers economic growth. However, most renewable energy sources face the challenge of intermittency. As reported by Colbertaldo et al. (2019), the major challenge in transitioning towards 100% renewable energy is the variable and intermittent behavior of renewable energy resources.

The increase of renewable energy integration into the current energy systems entails a necessity for large-scale energy storage systems to afford the variability and intermittency of renewable energy sources. The idea of renewable energy storage in an energy carrier such as hydrogen (Parra et al., 2019) which is storable, transportable, and utilizable is presented as a

solution. Hydrogen (H_2), a versatile not-carbon-containing fuel only generates water (H_2O) as a by-product when utilized for energy. Hydrogen has a high energy density which ranges from 120 to 142 MJ/kg and has the potential to tackle the overarching energy demand driven by fossil fuel consumption (Kim et al., 2021). Furthermore, hydrogen fuel has a variety of applications such as ammonia (NH_3) production, oil refining, methanol (CH_3OH) production, electricity generation, steel making, and fuel for transportation. Interest in hydrogen production is drastically gaining ground in recent years as it can be produced by several routes.

Hydrogen can be produced from fossil fuels as well as from renewable energy. Green hydrogen is the hydrogen produced without the emission of greenhouse gases into the atmosphere. Green hydrogen can be produced by using electricity from solar or wind through electrolysis of water giving oxygen as a by-product. It can as well be produced from biomass through biological and thermochemical processes. Biological processes include dark fermentation, photo-fermentation, bio-photolysis, and microbial electrolysis while thermochemical processes compose of gasification, pyrolysis, and steam methane reforming.

Biological processes are environmentally benign and constitute a potential for the efforts of shifting towards the development of clean alternative routes to attain sustainable hydrogen bio-based economy. Dark fermentative hydrogen production is an anaerobic digestion process that converts various renewable biomass resources including crop residues, food waste, agricultural residues, algal biomasses, organic fraction of municipal solid waste (MSW), and wastewater sludge into greenhouse gas-free hydrogen without the necessity of light. Dark fermentation is a relatively efficient route for biohydrogen production with the potential of becoming a cost-effective and reliable process in the near future. Certain lignocellulosic biomasses such as water hyacinth (WH) and banana peels (BP) are explored as potential feedstocks for dark fermentative hydrogen production.

Water hyacinth (WH), scientifically named Eichhornia crassipes is known as the world's most harmful and dreadful aquatic invasive plant (generates 14×10^7 daughter plants yearly) covering wide areas of water bodies (over 1.4 km^2) with about 28000 tons of fresh biomass content (Ruan et al., 2016). WH invasiveness disturbs aquatic systems and jeopardizes the livelihoods of people who practice economic activities on water bodies. In some areas, water hyacinths can cause dramatic floodings owing to the disturbance in water flow. It represents a serious hindrance to navigation, traffic, and recreation on water bodies. In Togo and

particularly in Lomé, the management of water hyacinth plants in the various lakes constitutes a heavy challenge for municipalities.

2. Problem statement

WH is regularly harvested from the lakes in Lomé to liberate space for fishing and navigation activities. WH removal from the lakes generates a lot of expenses for municipalities. The harvested WH is dumped or carried to a landfill which releases greenhouse gases into the atmosphere as shown in Figure 1. Banana peels are dumped on dumpsites which constitute a source of air pollution and bad smell.

Figure 1: a) WH plants in a lake in Lomé; b) Dumped WH undergoing decomposition; c) Banana fruits in the market, d) Banana peels

WH and BP (Figure 1) as biomasses in Lomé are not until present utilized for any major conversion to energy. Several studies have focused on the anaerobic fermentation of WH or BP for methane and/or hydrogen production (Cheng et al., 2010). Barua et al. (2019) reported the co-digestion of WH and BP for biogas production. Cheng et al. (2015) reported the production of fermentative hydrogen from hydrolyzed WH. Moreover, Nathoa et al. (2014) investigated the production of hydrogen and methane from BP by two-phase anaerobic

fermentation. However, the dark co-fermentation of WH and BP for hydrogen production has not been reported till recently.

3. Research questions

This research work is motivated by the following questions:

- What are the physicochemical properties of WH and BP biomasses for their biological conversion into hydrogen?
- What is the potential hydrogen yield of dark co-fermentation of WH and BP?
- What is the economic analysis of biohydrogen production from WH and BP in Lomé?
- What is the biogas yield of anaerobic digestion (AD) of WH, and BP?

4. Research hypotheses

The hypotheses guiding this research are formulated as follows:

- WH and BP physicochemical compositions favor a high hydrogen yield from their dark co-fermentation
- WH and BP regorge an important potential for biogas production

5. Objectives of the study

Given the lack of research regarding the anaerobic co-fermentation of water hyacinth and banana peels to generate hydrogen, this study generally aims to investigate the potential for hydrogen production by co-fermenting WH and BP biomasses. More specifically, it aims to:

- ✓ Characterize and analyze WH and BP biomasses
- ✓ Simulate hydrogen yield of different substrate's mixing ratios
- ✓ Evaluate the economic feasibility of fermentative hydrogen production from WH and BP in Lomé.
- ✓ Investigate biogas yield from the anaerobic digestion of WH and BP

6. Structure of the thesis

The study was structured into five parts. In the current part (Introduction), the context of the study and the problem have been exposed. The objectives as well as the research questions and hypotheses have been defined. In Part two (Chapter I), the available literature is reviewed to get more insights into hydrogen production via dark fermentation detailing the process metabolism as well as the process parameters. The chapter explores the literature on fermentative hydrogen production from WH and BP. Moreover, the chapter reviews the

concept of anaerobic co-fermentation and gives insights on bioprocess simulation using SuperPro Designer® software. Additionally, the chapter highlights the mechanism of anaerobic digestion process for biogas production. Part three (Chapter II) is consecrated to the methodology and materials applied for this study including the feedstock collection area, the feedstock characterization, simulation of the dark co-fermentation, economic and environmental analysis, and biogas production test methods. In Part four (Chapter III), the results are presented as well as the interpretation, discussions, and inferences. Part five (Conclusion, Summary, and Recommendations) concludes this work by providing a summary of key findings and some recommendations.

CHAPTER I: STATE OF KNOWLEDGE

I.1. Hydrogen production by dark fermentation

Fermentations are biochemical transformations occurring in aerobic or anaerobic environments and performing microbial decomposition of organic materials producing alcohols, hydrogen, acetone as well as CO_2 (Nikolaidis & Poullikkas, 2017). The products from fermentation depend on the catalyst used (isolated enzyme or microorganism producer) and fed organic substrate (mostly carbohydrate or protein) along with the process parameters. Rizwan et al. (2019) defined dark fermentation as the fermentation pathway carried out in the total absence of light and anaerobic conditions, where the breakdown of cellulosic organic feedstock results in the production of biological hydrogen along with organic acids and alcohols. Dark fermentation has been promoted for this study thanks to its cost-effectiveness, eco-friendliness, higher production rate, wider spectrum of substrates, and low energy requirement.

There are two main metabolic pathways in common for hydrogen production through dark fermentation: the formate pathway and the nicotinamide adenine dinucleotide (NADH) pathway as shown in Figure 2. The key factor in the formate pathway is the formate hydrogen lyase (FHL) complex. The core FHL complex comprises formate dehydrogenase (FDH) and hydrogenase (H_2-ase) (Figure 2). The FHL activates the oxidation of formate molecules and catalyzes the reduction of protons to generate hydrogen and carbon dioxide molecules. In the NADH pathway, the NADH molecules are consumed by oxidation to produce organic compounds. Ferredoxin (Fd)-NAD^+ reductase and ferredoxin hydrogenase are involved to generate hydrogen molecules through this pathway (Liu et al., 2017).

Hydrogen production by dark fermentation is governed by enzymes called hydrogenases. The two main hydrogenases phylogenetically different with different active sites are [FeFe]-hydrogenase and [NiFe]-hydrogenase. These enzymes are responsible for the reversible reaction of Equation (1). [FeFe]-hydrogenase operates in a complete anaerobic medium and generates more molecular hydrogen than [NiFe]-hydrogenase (Łukajtis et al., 2018).

$$2H^+ + 2e^- \leftrightarrow H_2 \quad (1)$$

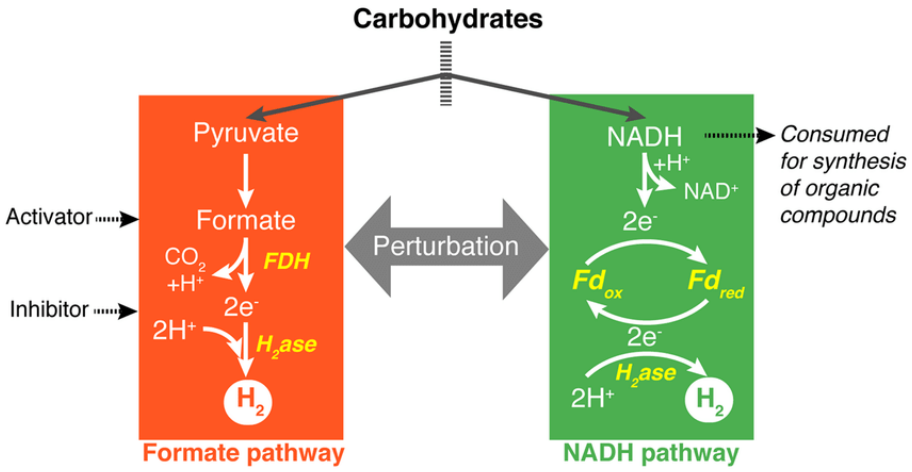

Figure 2: The two main metabolic hydrogen-producing pathways in dark fermentation: (Liu et al., 2017).

At present, the most common mechanism of hydrogen production by dark fermentation is glycolysis. Glycolysis is a mechanism in which metabolic processes involve glucose to produce hydrogen. In the glycolysis process, glucose is converted to pyruvate along with the formation of a reduced form of NADH, generating adenosine triphosphate (ATP) (Figure 3). In an anaerobic environment, pyruvate is converted into acetyl-Coenzyme A (Acetyl-CoA) in two ways. Pyruvate can be converted to acetyl-CoA through a reaction enabled by pyruvate ferredoxin oxidoreductase (PFOR) in the first pathway. This pathway ends with the production of molecular hydrogen through the reduction of [FeFe]-hydrogenase catalyzed by reduced ferredoxin (Fd). In the second pathway, pyruvate ferredoxin lyase enables the conversion of pyruvate to acetyl-CoA with the formation of formate. Formate can then be readily converted to hydrogen and carbon dioxide (CO_2) by [NiFe]-hydrogenase or [FeFe]-hydrogenase (Figure 3). Moreover, the NADH formed in the glycolysis step can be further converted to hydrogen in the presence of [FeFe]-hydrogenase (Qu et al., 2022).

The maximum theoretical hydrogen production per mole of glucose with respect to equation (2) is 12 mol (Osman, Deka, et al., 2020).

$$C_6H_{12}O_6 + 6H_2O \rightarrow 6CO_2 + 12H_2 \quad (2)$$

In practice, a maximum of 4 mol H_2 mol^{-1} glucose is achievable in the dark fermentation process (Sarangi & Nanda, 2020). The low H_2 yield is mainly due to the formation of by-products such as acetic acid, propionic acid, and butyric acid as shown in the equations (3), (4), (5) (Zagrodnik & Seifert, 2020).

$$C_6H_{12}O_6 + 2H_2O \rightarrow 2CH_3COOH + 2CO_2 + 4H_2 \quad (3)$$

(Acetic acid formation)

$C_6H_{12}O_6 \rightarrow CH_3COOH + CH_3CH_2COOH + CO_2 + H_2$ (4)
(Propionic acid formation)

$C_6H_{12}O_6 \rightarrow CH_3CH_2CH_2COOH + 2CO_2 + 2H_2$ (5)
(Butyric acid formation)

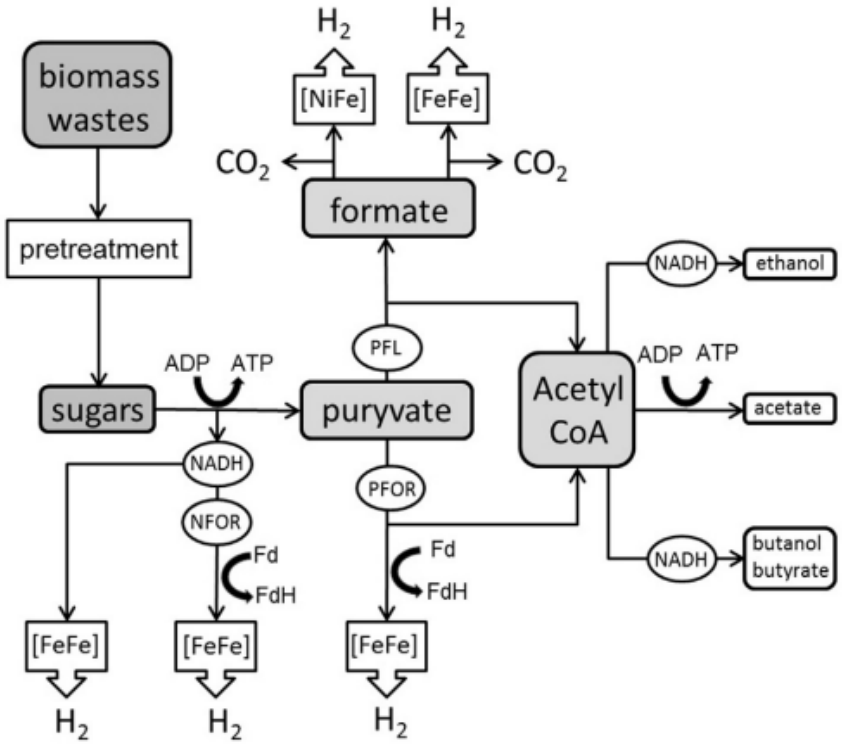

Figure 3: Mechanism of hydrogen production in dark fermentation of sugars (Łukajtis et al., 2018).

In recent days, several major advancements have been made to increase H_2 yield from dark fermentation. Such improvements include advanced approaches such as cell immobilization techniques, or metal ions and oxide nanoparticles (Mishra et al., 2019). The potential of nano-additive to the dark fermentation process and its impact on hydrogen productivity is a new area of research.

I.1.1. Factors influencing dark fermentation in a batch mode

I.1.1.1. The effect of pH

One of the most important parameters of dark fermentation is the pH value. pH influences the metabolic pathway, the microbial community, and the activity of microorganisms, thus affecting substrate degradation and product yield (X. Li et al., 2020; Soares et al., 2020). The control of pH and its maintenance at a constant optimal level is important in the fermentation

process. In fact, during fermentation, acids such as acetic, butyric, lactic, and propionic acid are produced and it lowers the pH of the medium, thus inhibiting the activity of hydrogenases. The pH keeps changing during fermentation and it should be noted that the optimum initial and operational pH depends on the kind of inoculum and substrate (Łukajtis et al., 2018). In general, it is found that the most extreme hydrogen yield and highest hydrogen production rate ranges from 5.0 to 7.0 corresponding to the range for bacterial growth (Kumar et al., 2017).

The control of pH is paramount to suppress the formation of methane gas in the bacterial sources of inoculum. Moreover, pH regulates hydrogen metabolism and drifts between solventogenesis and acidogenesis (Soares et al., 2020). So, the optimum pH (initial and operational) is critical for achieving high hydrogen production efficiency as pH is strictly dependent on the type of fed substrate, the structure of the reactor, and the composition of the microbial community (Vasmara et al., 2018).

I.1.1.2. Temperature

Temperature is an important parameter affecting microbial growth and the conversion efficiency in dark fermentation. In general, many components can be affected by temperature during fermentation, including the activity of enzymes such as hydrogenases, the degradation rate, the distribution of metabolite elements, and the composition of bacterial communities (Kothari et al., 2017; Zhang, 2021). Bacteria are classified into several temperature groups depending on their growth conditions: psychrophiles (10-20^{o}C), mesophiles (30-40^{o}C), and thermophiles (50-60^{o}C) (Weinrich et al., 2021). The selection of the optimum temperature may depend on the nature of bacteria used during fermentation for both mixed and pure cultures and the type of substrate used. Commonly, mesophilic temperatures are applied in the fermentation of most organic substrates. It is reported that higher temperatures catalyze the metabolism of enzymes responsible for hydrolysis, thus it is believed that thermophilic and extreme thermophilic temperatures are suitable for lignocellulosic substrates (Wong et al., 2014). Because mesophilic bacteria are incapable of using cellulose directly to generate hydrogen, they need an intermediate exogenous cellulase to involve while thermophilic bacteria convert cellulose directly to hydrogen. The disadvantage of thermophilic temperatures is the higher energy consumption which decreases the profitability of the process. According to several studies, mesophilic temperatures around 35-40^{o}C are most applied in dark fermentation (Jain et al., 2022).

I.1.1.3. Micro-organisms

Micro-organisms play a key role in fermentation processes. Specific microorganisms are involved in the dark fermentation process to enhance the hydrogen content in the output gas mixture. Fermentative hydrogen production is achieved by various micro-organisms capable of digesting a wide range of organic substrates. The most used mesophilic cultures for H_2 production are Clostridium and Enterobacter (Clostridium Beijerinckii, Clostridium butyricum, Enterobacter aerogenes, and Enterobacter asbiriae) whereas the commonly used thermophilic one is Thermoanaerobium (Thermoanaerobacterium thermosaccharolyticum) (Haque et al., 2022). Moreover, with regard to their growth of metabolism in aerobic conditions, they are considered facultative (e.g. E.cloacae, Enterobacter aerogenes, Citrobacter intermedius, and Escherichia coli) or obligate (strict) bacteria (e.g. C. parafutricum, Rumunococcus albus, Clostridium butyricum, and Clostridium beijerinckii) (Chandrasekhar et al., 2015). Strict anaerobes are very sensitive to oxygen. With strict anaerobes, a tiny amount of oxygen in the fermentation medium completely inhibits the H_2-producing activities while facultative anaerobes consume oxygen quickly, creating anaerobic conditions in the medium (Soares et al., 2020). Thus, biohydrogen production using facultative bacteria would be more cost-effective than using obligate bacteria.

However, the presence of some hydrogenotrophic methanogens in the fermentation medium constitutes a headwind for the dark fermentation process. Those methanogens act as one of the major H_2-consuming micro-organisms reducing the H_2 yield by consuming H_2 to increase methane yield (equation (6)). Pre-treatment of inoculum is applied for enriching H_2-producing bacteria and eliminating H_2-consuming methanogens (Rafieenia et al., 2018).

$$4H_2 + CO_2 \rightarrow CH_4 + 2H_2O \quad (6)$$

I.1.1.4. Hydraulic retention time (HRT)

Another important parameter to be considered in dark fermentation is the hydraulic retention time (HRT). Santiago et al. (2020) found that HRT and solid retention time (SRT) have a heavy impact on biohydrogen production and associated by-products from organic solid waste (OSW) through the dark fermentation process. HRT corresponds to the average length of time that a fed substrate is kept in the fermentation reactor. The hydrogen production rate increases within a certain range of time but after surpassing the optimum HRT, the production rate diminishes with an increase in HRT. Lu et al. (2019) studying the effects of HRT and concentration of substrate on hydrogen production rate (HPR) from glucose, reported that a

maximum HPR of 100.2 mol m^{-3} was achieved daily at an HRT of 24 h and substrate concentration of 30 g L^{-1}. The HRT depends on the type of substrate and its biodegradability, and the type of reactor. Many studies in the literature have investigated the impact of HRT on hydrogen production yield. Santiago et al. (2019) evaluated the influence of HRT (8 to 48 h) on hydrogen production behavior and microbial community during dark fermentation of food waste. They reported that the highest hydrogen content (23.2 %) in the biogas was obtained at an HRT of 48 h. The decrease in HRT led to an increase in hydrogen production rate (HPR) but decreased hydrogen content in the biogas. A microbial analysis revealed that Clostridium sp. was predominant at an HRT of 48 h while Enterobacter and Lactobacillus were abundant between HRTs of eight and 48 h.

I.1.1.5. Substrate

Fermentative hydrogen production is influenced by the substrate type and its concentration in the reactor. In the case of batch fermentations, the food-to-micro-organism ratio (F/M) is paramount in the operation of a reactor. An appropriate F/M ratio is essential to avoid stagnation of substrate and its inhibition. A higher F/M ratio leads to the accumulation of volatile fatty acids (VFAs), decreasing thus the pH and affecting hydrogen yield.

Moreover, substrate concentration is an important factor for hydrogen yield in dark fermentation. The highest hydrogen yields are usually obtained for diluted substrates with concentrations ranging from 10 to 20 g L^{-1}. However, higher total volumes of hydrogen are obtained from higher-concentration substrates (Łukajtis et al., 2018).

Several types of substrates have been explored for biohydrogen production by dark fermentation. These substrates include lignocellulosic substrate, organic wastes, starch, and wastewaters as well as pure sugars such as glucose, xylose, and sucrose (Sevilimedu Veeravalli, 2014; Zhang, 2021). Each type of substrate has its characteristics, and this has a heavy impact on the hydrogen production output. However, the use of pure sugars is related to first-generation biofuel production; it competes with food and thus jeopardizes efforts for sustainable development.

I.1.1.6. Nutrients

Bacteria growth and activity are highly affected by the availability of macro- and micro-nutrients in the medium. Carbohydrates constitute the major source of nutrients but there are other nutrients (inorganic) such as nitrogen, and phosphorus that are essential for microbial growth and activity. However, higher proportions of inorganic nutrients may inhibit the

activity of micro-organisms. For instance, high ammonical nitrogen concentration and high C/N ratio in feedstock inhibit the fermentation process (Kothari et al., 2017). Nitrogen-induced inhibition is more encountered with organic substrate obtained from animal manure which is rich in ammonical nitrogen. Anaerobic bacteria consume carbon faster than nitrogen during fermentation. So, it is required adequate balancing of the C/N ratio to prevent the inhibitory effects of nitrogen. It is reported that pure substrates such as glucose, xylose, and starch demand a low nitrogen content with a C/N ratio ranging from 137 to 200 while mixed substrates such as lignocellulosic substrate, food waste require a high nitrogen concentration with a C/N ratio ranging from four to 50 (Argun & Onaran, 2017; Pérez-Rangel et al., 2020; Soltan et al., 2019).

Phosphorus is another essential macro-nutrient for dark fermentation and can be added to the process as phosphate. Optimum phosphorus concentration improves cell growth and contributes to high-yield hydrogen production (Xu et al., 2016). The literature regarding phosphorus concentration for hydrogen production reported that pure substrates require lower phosphorus addition with the optimum C/P ratio ranging from 700 to 1000 while for complex substrates, the C/P ratio ranges from 11 to 559 (Argun & Onaran, 2017; Carosia et al., 2017).

I.1.2. Inoculum for dark fermentation

Hydrogen production is facilitated by specific bacteria that are mostly supplemented to the fermentation medium. Contrary to conventional anaerobic processes, fermentative hydrogen production hardly occurs with only endogenous microorganisms. There is always a need for supplementary bacteria to enable the hydrogen-producing processes. These bacteria can be from pure culture or mixed culture microorganisms.

I.1.2.1 Pure cultures

Pure cultures are isolated grown bacterial strains that can be introduced into a dark fermentation medium to enhance hydrogen-producing activity. Recently, pure culture selection for the improvement of hydrogen-producing fermentation processes is extensively investigated (Policastro, Carraturo, et al., 2022). The common pure cultures applied in dark fermentation are Enterobacter and Clostridium species. Enterobacter aerogenes as facultative bacteria consume oxygen in the medium and generate a high hydrogen production rate (HPR) and bacterial growth whereas Clostridium acetobutylicum, sensitive to oxygen generates a higher hydrogen yield (Jayachandran & Basak, 2023). Clostridium bacteria are known to be more efficient than Enterobacter species. Jayachandran & Basak (2023) reviewed that

theoretically, Enterobacter species produce two (02) mol H_2 mol^{-1} glucose while Clostridium species produce four (04) mol H_2 mol^{-1} glucose. Many other pure cultures such as Escherichia Coli, Clostridium butyricum, are explored for enhancing biohydrogen production.

I.1.2.2. Mixed cultures

Mixed cultures are many bacterial strains existing in synergy to consume the substrate and release hydrogen. Mixed cultures have several advantages such as bacterial diversity, consumption of complex substrates, reduction of inhibitory compounds, diverse metabolism pathways, and higher hydrogen production rate (Hasibar et al., 2020; R. Wang et al., 2020). A mixed culture strategy is an innovative approach to scaling up biohydrogen production processes. Mixed cultures have been reported in many papers as a promising solution for high-yield hydrogen production (Ohnishi et al., 2022; Sivagurunathan & Lin, 2020).

I.2. Fermentative hydrogen production from water hyacinth and banana peels

Hydrogen production by fermentation of lignocellulosic biomass material, specifically water hyacinth and banana peels has been explored in recent years. Water hyacinth as well as banana peels have attractive physicochemical characteristics that give them the potential to produce hydrogen through dark fermentation.

I.2.1. Water hyacinth as a substrate for biohydrogen production

Water hyacinth (WH) as a widely extensive aquatic plant, can be valorized into hydrogen. Research has been carried out to characterize WH biomass to appreciate its possible valorization into energy products. Wauton & William-Ebi (2019) conducted research on the characterization of WH for the production of thermochemical fuels. They reported that WH had the following composition (wt%): 71.27% of volatile matter (VM), 14.56% of fixed carbon, 14.56% of ash content, 28% of hemicellulose, 26% of cellulose, and 6% of lignin. This composition shows that WH is rich in volatile matter and carbohydrates that are necessary for hydrogen production by dark fermentation. WH's physicochemical properties, fast growth, and availability make it a suitable substrate for biohydrogen production.

Studies showed that dark fermentation of water WH resulted in a high hydrogen yield. Most of the studies dealt with a thermochemical pretreatment of WH before the fermentation phase. Mechery et al. (2017) reported that alkali (NaOH) pretreatment of WH resulted in a higher hydrogen yield than acidic (H_2SO_4) pretreatment in the dark fermentation process. The chemical pretreatment facilitates the hydrolysis of cellulose and hemicellulose, and the

delignification of WH. Su et al. (2010) reported hydrogen production from WH through dark and photo-fermentation. They mentioned that 20 g L^{-1} of WH was pretreated with steam heating and alkali which resulted in 76.7 mL H_2 g^{-1} VS after the dark fermentation step. Elsamadony & Tawfik (2018) reported a hydrogen yield of 119.6 mL g^{-1} H_2 from the dark fermentation of WH after adding sodium chlorite ($NaClO_2$) to the fermentation medium. On the same principle, Wazeri et al., (2018) used mixed culture supplemented with sodium bicarbonate ($NaHCO_3$) to achieve 69±4.3 mL g^{-1} VS hydrogen yield from dark fermentation of WH.

I.2.2. Banana peels as a substrate for biohydrogen production

Banana peel (BP) waste is a lignocellulosic biomass that incorporates interesting components for biohydrogen production. Kabenge et al. (2018) carried out the characterization of BP waste as a potential slow pyrolysis feedstock. They found that BP had the following properties: 88.02% volatile matter, 18.38 C/N, 58.08% organic matter, 41.38% hemicellulose, 9.9% cellulose, and 8.9% lignin (wt%). These properties set BP as a favorable substrate for biohydrogen production.

Nathoa et al. (2014) experimented with the cogeneration of hydrogen and methane in two-stage dark fermentation of BP and found hydrogen yield to be 209.9 mL g^{-1} VS in the dark fermentation step. Lara et al. (2020) evaluated hydrogen production in a batch bioreactor using Clostridium butyricum DSM 2478 from BP and found about 668.4 mmol H_2 L^{-1}. Moreover, recently Ahmad et al. (2022) reported the production of bio-hydrogen from banana waste by using anaerobic fermentation. In the previous study, acidic (H_2SO_4) and alkali (NaOH) pretreatment were applied to 10g of a substrate and achieved a hydrogen yield of 78 mL after 384 h HRT. Fermentative hydrogen production from the BP is a promising route. However, the co-fermentation of BP with WH could be a better option for hydrogen production as research has still not highlighted this approach. Hence, this study seeks to bring a response to this shortage.

I.3. The concept of anaerobic co-fermentation

Co-fermentation is defined as an organic substrate processing method that consists of mixing and fermenting together two or multiple substrates with complementary characteristics for biofuel production. Co-fermentation improves process stability and biodegradation performance of organic material while optimizing biofuel yield (Soeprijanto et al., 2021). Soltan et al. (2019) reported that dual- and multi-fermentation balance macro- and micro-

nutrients at their ideal levels which reflects on bacterial performance and therefore optimizes hydrogen yield. To overcome the inhibiting effect of olive mill wastewater containing recalcitrant/toxic compounds and cheese whey, lacking pH buffering capacity, Policastro et al. (2022) experimented with the co-fermentation of both substrates and reported a high hydrogen yield. Dual and multi-fermentation are required for balancing nutrients hierarchy which maximizes hydrogen potential through batch fermentations.

Yang et al. (2019) performed the co-fermentation of fallen leaves and sewage sludge for the production of hydrogen at different mixing ratios and reported that the co-fermentation process had shown a synergistic effect on the biohydrogen yield. This effect is caused by the increase and enrichment of the microbial community. Recently, Barua et al. (2019) explored the anaerobic co-digestion of water hyacinth and banana peels with and without thermal pre-treatment and reported that this process portrayed a synergistic action on the biogas production by balancing the overall process. Fermenting two or more substrates is a gaining strategy for improved biohydrogen production processes.

I.4. Bioprocess simulation using SuperPro Designer®

SuperPro Designer® (SPD) is a software tool that provides modeling, assessment, and optimization of integrated batch and continuous processes across industries such as Biotech, Pharmaceutical, Specialty Chemical, Food Processing, Consumer Goods, Metallurgical, Materials, Water Purification, Wastewater Treatment, Air Pollution Control, etc. The software is equipped with a combination of manufacturing and environmental operation models which enable users to simultaneously design and optimize manufacturing and end-of-pipe treatment processes and practice pollution prevention and control (Intelligen, Inc.). SPD is known as one of the best options for biochemical or environmental engineers and scientists in R&D. Moreover, SPD provides outputs such as material and energy balances of integrated processes, equipment sizing, cost analysis, economic evaluation, environmental impact assessment, and many more.

Computational methods can be used in bioprocesses to observe system behavior and evaluate the output of a given process. The SPD software runs on three reaction models (Bergman, 2016):

- Stoichiometric: the time dependence is only set by the temperature
- Equilibrium: the equilibrium constants determine the extent of the stoichiometric reactions

- Kinetic: kinetic parameters are entered into a selection of pre-defined models.

For this study, kinetic models were used. In SPD, the kinetic growth is represented by equation (7) where Qc (g L^{-1} h^{-1}) is the volumetric productivity of component C, μ_{max} the maximal growth of cell biomass, S is the possible models integrated into SPD, X is the concentration of the biomass (g L^{-1}), α and β experimentally determined coefficients.

$$Q_c = (\alpha \times \mu_{max} \times S_1 \times S_2 \times S_3 + \beta) \times X \quad (7)$$

Several studies used SPD to simulate biological processes. Bergman, (2016) used SPD to simulate biohydrogen production by dark fermentation of potato peels. In the mentioned study, they additionally simulated the economic analysis of such a process. Moreover, Koók et al., (2014) simulated biohydrogen production from glucose using SPD and they obtained over 20 mol H_2 for an HRT of 9 h after two purification steps.

I.5. Biogas production process

I.5.1. The concept and the metabolism of anaerobic digestion

Biogas is a renewable and environmentally friendly gaseous fuel, produced by anaerobic digestion (AD) of organic materials such as biomass, waste resources, industrial effluents, and wastewater sludge. Anaerobic digestion (AD) is a biological process by which particulate organic matter is broken down into its simple soluble forms thanks to a robust microbial community in the absence of oxygen, releasing thus biogas (Barua, 2018). Raw biogas is mainly composed of methane (50-75%), carbon dioxide (25-50%), a small amount of nitrogen (2-8%), and trace components such as hydrogen, hydrogen sulfide, ammonia, and several organic volatile compounds depending on the feedstock (Y. Li et al., 2019).

The AD for biogas production generally consists of four stages: Hydrolysis, acidogenesis, acetogenesis, and methanogenesis. All the stages are interconnected as well as the bacterial consortium operating through them. In this interrelation, the products of one stage become the substrates of the following stage, and so on.

- Hydrolysis: In this step, long-chain organic polymers such as proteins, lipids, and polysaccharides are broken down into simple soluble monomers such as sugars, glycerol, amino acids, fatty acids, etc. by hydrolytic bacteria.
- Acidogenesis: at this stage, acidogenic bacteria (facultative and obligate) convert the products of hydrolysis into organic acids or volatile fatty acids (VFAs), alcohols, and inorganic compounds such us H_2, H_2S, CO_2, and NH_3.

- Acetogenesis: here, mainly hydrogen, CO_2, and acetate are produced from the products of acidogenesis by acetogens and hydrogenases.
- Methanogenesis: this step marks the end of the AD process through the production of methane from the products of the acetogenesis process, assisted by acetotrophic and hydrogenotrophic methanogens (Richard et al., 2019). Figure 4 summarizes the different steps of AD.

I.5.2. Biogas production from water hyacinth and banana peels

In the last decade, research has focused on the anaerobic digestion of water hyacinth, and banana peels as potential substrates for biogas production. Hudakorn & Sritrakul (2020) reported methane yield to be 237 mL CH_4 g^{-1} VS from the anaerobic digestion of WHL and WHS juice at a F/M ratio of 1:1. Moreover, Nugraha et al. (2018) reported that up to 151.548 mL g^{-1} VS of biogas can be obtained from water hyacinth at a F/M ratio of 10.01. Recently, Manigandan et al. (2023) examined the effect of pretreatment on biogas production from various WH samples. They reported that treated WH samples exhibited higher biogas yield with the maximum cumulative yield reaching 209 mL on the 19^{th} day. So, WH is an ideal candidate for biogas production. Achinas et al. (2019) reported a maximum biogas yield of 112.18 mL g^{-1} VS from the batch anaerobic digestion of BP at the concentration of 10g VS L^{-1} with 10% cow manure as inoculum. WH and BP could be potential substrates for higher biogas production, in this regard, this study seeks to assess the potential for biogas production from WH and BP.

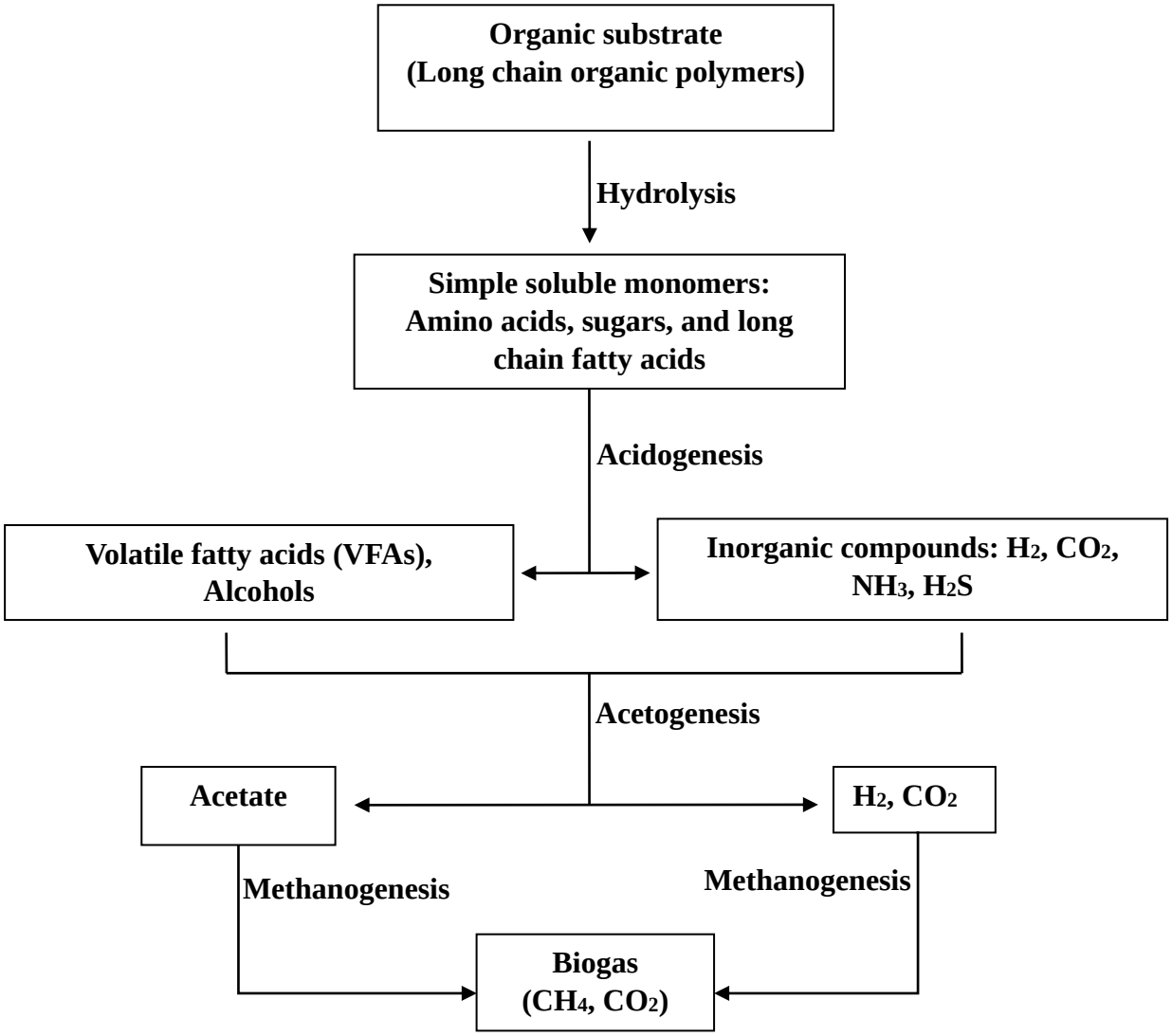

Figure 4: The different stages of anaerobic digestion of organic waste (modified from Barua (2018))

II.1. Methodology of data collection and materials

II.1.1. Materials and sample collection area

Water hyacinth plants of the species of *Eichhornia Crassipes* were harvested from the shores of the lake known as Lac Ouest in Lomé using a machete. The collected water hyacinth was then transported in a nylon bag to the laboratory for subsequent treatments.

To get the peels, a basket of banana fruits of the species of *Musa Acuminata Cola*, was bought from the fruits market of Hanoukopé, in Lomé. The banana fruits were then transported in a plastic bag to the hostel where it was eaten and the peels were collected to the laboratory for pre-treatment. The map of the sample collection area was designed using the software application MAPS.ME and the software QGIS as displayed in Figure 5.

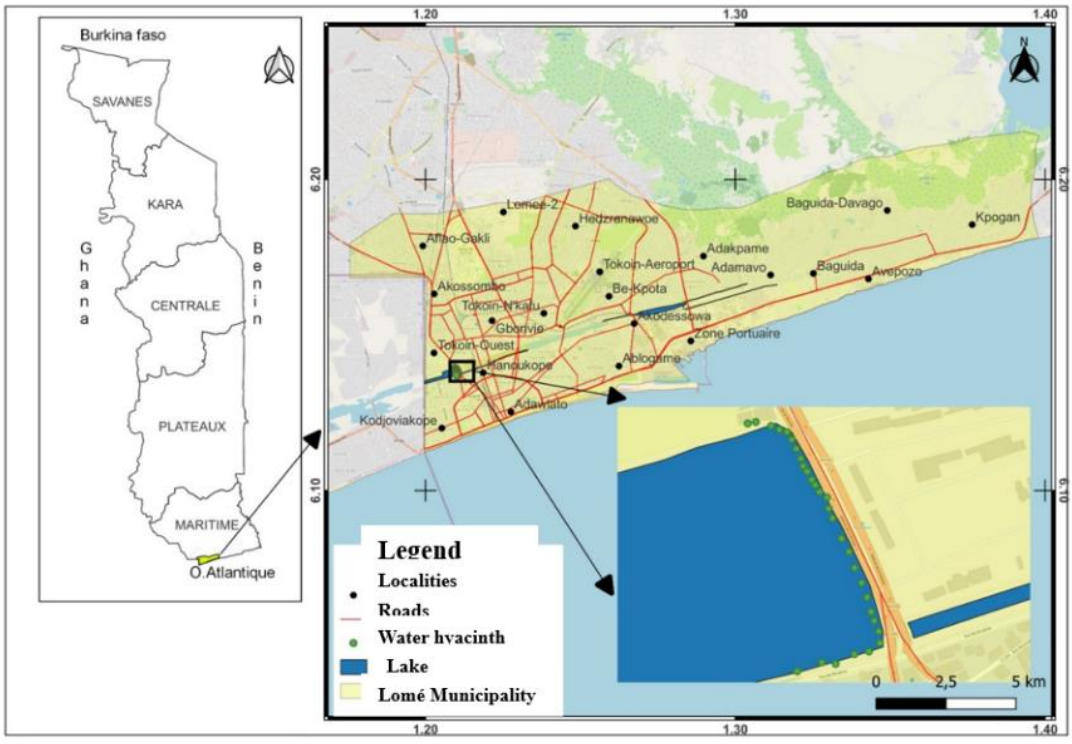

Figure 5: Water hyacinth collection site on the shore of the Lac Ouest, Lomé, Togo (MAPS.ME and QGIS)

II.1.2. Sample pre-treatment and preparation

The collected WH plants were washed in a bucket using tap water and then rinsed with distilled water to ensure inhibitory particles are removed. The WH was subsequently dried naturally in the sunlight using a plastic carpet for seven days. The BP were also dried in the

sunlight for seven consecutive days. After sun drying, the WH was separated into roots, stems, and leaves using a medium size scissors. The separation was done after sun-drying to avoid losses of critical substances from the fresh sample. The samples of WH parts and BP were then dried in an oven (INTERLABS INSTRUMENT, DP1-I) using two aluminum dishes for 24 h at the temperature of 105^{o}C. The dried samples were ultimately ground using a mortar and a pestle to reduce to a particle size of approximately three millimeters. The ground samples were then stored in air-tight plastic bottles for subsequent experiments. The diagram of the whole pretreatment process can be found in Appendix A.

II.2. Research approach and design

The research approach for this study is dissected into four parts: the first part deals with the extensive characterization of the different samples, the second part covers the simulation methods and procedure using SPD, the third part concerns the economic feasibility study, and the last part describes the methods for the biogas production test of the samples.

II.2.1. Characterization methods and materials

II.2.1.1. Ultimate analysis

The elemental analysis of the samples was carried out using Laser Induced Breakdown Spectroscopy (LIBS) to detect the content of chemical elements that compose water hyacinth and banana peel biomasses. A small amount of each sample (WHL, WHS, WHR, and BP) was placed under an optic microscope (KEYENCE VHX-7000) using an aluminum sample bowl. The sample under the optic microscope was then scanned and the plasma was analyzed by the LIBS analyzer (VHX-7000). A multi-points line analysis was done on each of the samples as shown in Figure 6. The different steps are shown in Appendix B.

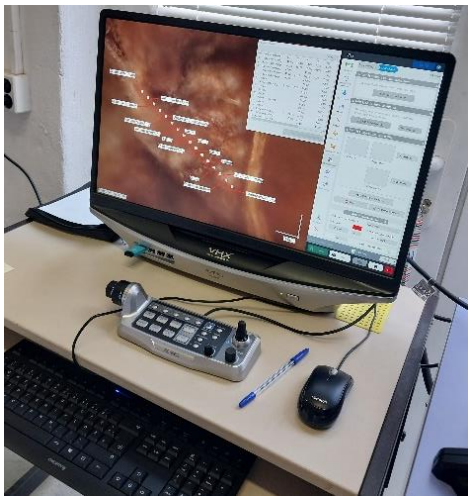

Figure 6: A multi-points line analysis of WHL using LIBS analyzer (VHX-7000)

II.2.1.2. Proximate analysis

The proximate analysis was performed with respect to the standard DIN EN 15935 (2012-11) (Jan Liebetrau & Pfeiffer, 2020). Fresh samples of WH and BP were collected in two aluminum dishes and weighed on a kitchen scale (m_f). After weighing, the two samples were successively dried in the sunlight for 7 days and in the oven (INTERLABS INSTRUMENT, DP1-I) at 105°C for 24 h. The final masses of the samples after oven-drying were recorded (m_d). The moisture content (MC) and the total solid (TS) were calculated using equations (8) and (9).

$$MC = \frac{m_f - m_d}{m_f - m_{dish}} \times 100 \quad (8)$$

$$TS = \frac{m_d - m_{dish}}{m_{f-m_{dish}}} \times 100 \quad (9)$$

With m_f=fresh mass with the dish, m_d=dried mass with the dish, m_{dish}=mass of the dish.

Another sample of WH was dried using sunlight for seven days. After sun-drying, the mass of the sample was recorded (m_{sample}). Then the sample was separated into roots, stems, and leaves as explained previously. The mass of each part was recorded. The mass percentage of each part was calculated using equations (10-12).

$$\%\_WHL = \frac{m_{WHL} - m_{dish}}{m_{sample} - m_{dish}} \times 100 \quad (10)$$

$$\%\_WHS = \frac{m_{WHS} - m_{dish}}{m_{sample} - m_{dish}} \times 100 \quad (11)$$

$$\%\_WHR = \frac{m_{WHR} - m_{dish}}{m_{sample} - m_{dish}} \times 100 \quad (12)$$

With m_{WHL}=weight of WHL; m_{WHS}=weight of WHS, m_{WHR}=weight of WHR, %_WHL=share of WHL, %_WHS=share of WHS, and %_WHR=share of WHR.

The stored ground samples were brought to Rostock, Germany for analysis and experiments. Three samples of each substrate (WHL, WHS, WHR, and BP) were taken in different crucibles and their weights were recorded (m_f) using a weigh scale (KERN, ABT 320-4M). The crucibles with the samples were dried in an oven (BINDER) at 105°C to a constant weight. The constant weights of the crucibles with the dried samples were recorded (m_d). Subsequently, the samples were calcinated in a muffle furnace (Venticell, Armin BAACK, Labortechnik) at 220°C for 30 min at first, and then for two hours at 550°C. After the

incineration, the hot crucibles were cooled down in a desiccator. After the cooling down of the crucibles, their weights were recorded (m_{ash}). Equations (13-16) were used to determine the volatile solid (VS), the ash content (AC), the moisture content (MC), and the total solid (TS) of the samples.

$$MC = \frac{m_f - m_d}{m_f - m_{crucible}} \times 100 \quad (13)$$

$$\mathrm{TS} = \frac{m_d - m_{crucible}}{m_{f-m_{crucible}}} \times 100 \quad (14)$$

$$\mathrm{VS} = \frac{m_d - m_{ash}}{m_{d-m_{crucible}}} \times 100 \quad (15)$$

$$\mathrm{AC} = \frac{m_{ash} - m_{crucible}}{m_{d-m_{crucible}}} \times 100 \quad (16)$$

II.2.1.3. Fiber analysis

The fractions of cellulose, hemicellulose, and lignin of the parts of WH and BP were investigated according to Weende Method (crude fiber). The method consisted of determining the neutral detergent fiber (NDF), the acid detergent fiber (ADF), and the acid detergent lignin (ADL) after washing samples with chemical solutions. Fibrebags were used and their empty weights were recorded (m_1). Then one g of each sample was put in the Fibrebags and the mass of the Fibrebag with the sample was recorded as m_2. A glass spacer was introduced into the Fibrebag and both were placed in a sample carousel. Then all the Fibrebags were plunged for 5min in a beaker containing about 300 mL acetone solution to remove fats. Afterward, the samples were placed in a Fibretherm FT 12 to be washed with 1.3 L ADF solution (distilled water + Sulfuric acid + N-cetyl-N,N,N-trimethyl ammonium bromide). After completion of the Fibretherm operations, the samples were dried in an oven (BINDER) overnight at 105°C and their mass with crucible was recorded (m_4). The mass of the empty crucible was recorded as m_3. Afterward, the Fibrebags were ashed at 500°C for two h in the muffle furnace (Venticell, Armin BAACK, Labortechnik). After cooling down in a desiccator, the weights of the samples with the crucible were recorded as m_5.

For the ADL determination, the dried samples (m_4), were hung in the carousel and secured. Subsequently, the carousel with the Fibrebags was placed in a five liters beaker and covered at room temperature with 72% sulfuric acid. The fibrebags were then rinsed with hot water to the neutral point and dried for 24 h at 105°C and their mass was recorded as m_7.

Similarly, for the NDF determination, after the fats' removal and drying of the samples for approximately two minutes in the exhaust, the Fibertherm was started to wash the samples with NDF solution. After the Fibretherm was completed, the spacer was carefully removed from each Fibrebag. Then the Fibrebag with the sample was rolled up and placed in the crucible and dried at 105°C for 24 h (m_8). Subsequently, the Fibrebag containing the sample was ashed at 500°C and cooled down, the weigh recorded (m_9). The share of the different components was calculated using equations (17-22) (Jan Liebetrau & Pfeiffer, 2020). See Appendix C for the materials involved in the process.

$$ADF = \frac{(m_4 - m_1) - \left(m_5 - (m_6 - m_3)\right)}{((m_2 - m_1) \times TS \times 100 \times 100} \quad (17)$$

$$ADL = \frac{(m_7 - m_1) - \left(m_5 - (m_6 - m_3)\right)}{((m_2 - m_1) \times TS) \times 100 \times 100} \quad (18)$$

$$NDF = \frac{(m_8 - m_1) - \left(m_9 - (m_6 - m_3)\right)}{((m_2 - m_1) \times TS) \times 100 \times 100} \quad (19)$$

%_Hemicellulose=NDF-ADF (20)

%_Lignin=ADL (21)

%_Cellulose=NDF- (Hemicellulose + Lignin) (22)

ADF=share of acid detergent fiber (%TS), ADL=share of acid detergent lignin (%TS), NDF=share of neutral detergent fiber (%TS)

II.2.2. Simulation methods and procedure in SuperPro Designer®

SuperPro Designer® (SPD) version 13 build 2 (V13.2) was used as the software material for the simulation. Two (02) unit procedures were set up in the software: a fermentation unit and an absorption unit.

A fermenter was set up and supplied with the substrates (WHL and WHS), the co-substrate (BP), water, an inoculum, and a hydrolase enzyme. For the substrates, three stock mixtures were created in SPD: water hyacinth leaves (WHL), water hyacinth stems (WHS), and banana peels (BP) stock mixtures (Table 1). A constant mass ratio of 65:35 was set between WHS and WHL on one hand, and on the other hand four (4) varying water hyacinth (WHL + WHS) to banana peels mass ratios such as 100:0, 0:100, 50:50, and 70:30 was investigated (Table 2). All the mixing ratios were based on VS content.

Table 1: Composition of the different stock mixtures

Component	WHL (wt%)	WHS (wt%)	BP (wt%)
Cellulose	18.73	27.08	11.71
Hemicellulose	25.73	18.4	10.37
Lignin	5.08	4.47	21.03
Other solids	50.46	50.05	56.89

Table 2: Mixing ratios and mass of the substrates

Mixing ratio		Water hyacinth		Banana peels(kg)
VS basis	Fresh matter basis	WHL(kg)	WHS(kg)	
100:0	100:0	1012.2	2077.41	0
0:100	0:100	0	0	2791.56
50:50	52.5:47.5	506.11	1038.71	1395.78
70:30	72.1:27.9	708.54	1454.19	837.47

A volume of 10,000 L of water was added to each substrate to achieve a substrate concentration of 225 g VS L^{-1}. For the simulation, the quantities of hydrolase and inoculum did not account. So, 10kg was taken for each. A volume of five liters of nitrogen was flushed in the fermenter to create the anaerobic condition.

All the inputs to the fermenter were charged at a temperature of 25^{o}C, 1 atm. The fermenter was heated and maintained at 37^{o}C, 1 atm. The different unit operations in this unit procedure were: charge operations for the inputs, heating operation, stoichiometric fermentation, kinetic fermentation, and transfer out operation. The hydraulic retention time (HRT) was 24 h. A series of reactions took place in the fermenter upon the following approximations:

- Water does not evaporate in the fermenter
- The produced gases do not dissolve
- Materials are not left in the fermenter
  - Stoichiometric fermentation: Hydrolysis of hemicellulose and cellulose

The reactions are summarized in Table 3.

Table 3: Stoichiometric fermentation reactions with their conversion efficiencies

Reaction	Conversion coefficient
Cellulose + Water → Glucose	90%
Hemicellulose + Water → Xylose	50%

- Kinetic fermentation: conversion of glucose into hydrogen and by-products

The Monod-model was adopted for the fermentation kinetics (equation 23).

$$\mu = \mu_{max} \frac{[S]}{K_s + [S]} \quad (23)$$

μ is the specific growth rate, [S] is the concentration of the limiting substrate for growth, and Ks is the half-saturation constant.

The equations of the different kinetic reactions that occur inside the fermenter and the values of their parameters are found in Table 4.

Table 4: Equations of kinetic reactions and the values of their parameters in the Monod-model

Reaction	μ_{max} (h^{-1})	Ks (mg L^{-1})	Reference
$C_6H_{12}O_6 + 6H_2O \rightarrow 6CO_2 + 12H_2$ (24)	0.05	35	(Koók et al., 2014)
$C_6H_{12}O_6 + 2H_2O \rightarrow 2CO_2 + 2CH_3COOH + 4H_2$ (25)	0.125	35	(Mata-Alvarez, 2003)
$180C_6H_{12}O_6 \rightarrow$ 73.2g Biomass + 106.48gCO_2 (26)	0.20	35	(Bergman, 2016)

After the fermentation process was ended, the content of the reactor was transferred out. The gas mixture was expelled through the vent and transferred in an absorption reactor at 1 atm, 37°C. 100 L of water was supplied to the absorption vessel. After the absorption of impurities, hydrogen was transferred out through the exhaust gas port whereas the impurities with water flowed out through the outlet. Figure 7 shows the process flowsheet. The cumulative hydrogen yield was calculated using the formula of equation (27).

$$H_{2yield} = \frac{m_{H2}}{\rho_{H2} \times m_{TVS}} \quad (27)$$

ρ_{H2}=density of H_2 in standard conditions (g mL^{-1}), m_{H2}=mass of cumulative H_2(g), m_{TVS}=mass of total volatile solid of the substrates (g), H_{2yield}=Hydrogen yield (mL g^{-1} VS).

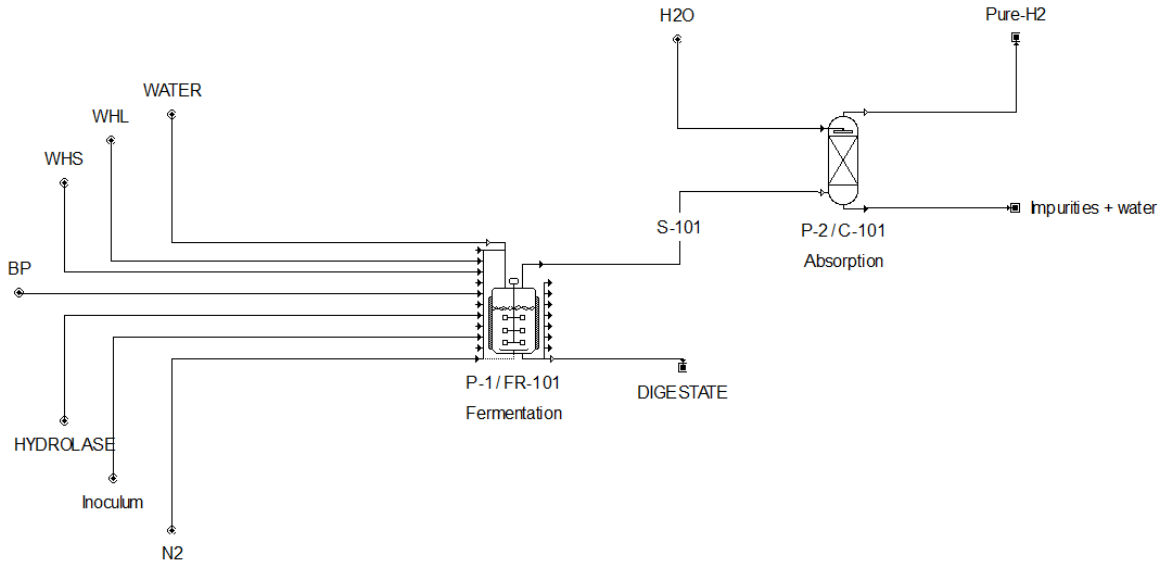

Figure 7: The flowsheet of the dark co-fermentation process in SPD

II.2.3. Economic and environmental analysis

To better apprehend the economic feasibility of fermentative hydrogen production from WH and BP in Lomé, two main scenarios were established: WH to landfill, and WH to hydrogen. A comparative analysis was made between the two scenarii.

II.2.3.1. Scenario 1: Water hyacinth and banana peels into landfill pathway

This scenario describes the current state of WH and BP waste management in Lomé. In this approach, WH is harvested and transported straight to the landfill. WH is harvested mechanically by using mechanical tools and machines. Based on the study of Z. Wang et al. (2019), it was assumed that the average harvest cost of WH is equal to 2 USD ton^{-1} (1,241 FCFA). The workers for WH collection were paid 2 USD ton^{-1}.

For BP waste, it was assumed that there was a banana fruit processing plant where a large amount of BP waste was generated. The BP were considered to be collected for free and only the transportation cost was applied to it. As reported by Z. Wang & Calderon (2012), a truck carrying five (05) tons per trip consumes four (04) liters of diesel. One liter of diesel cost 1.30 USD (800 FCFA). So, the cost of both WH and BP transportation was estimated at 1.04 USD ton^{-1}. The Driver was paid 1.6 USD ton^{-1} (992 FCFA). For comparison reason, it was assumed that both the landfill and the biohydrogen plant would locate in the same place where a truck transportation of the feedstock would only require four (04) liters of diesel to minimize transportation cost. The summary of expenses is found in Table 5.

For greenhouse gas (GHG) emissions, it was assumed that the same quantity of CO_2 would be emitted for WH and BP collection and transportation in the two (02) scenarii. So, for comparison issue, the boundary of the life cycle analysis was considered from the landfill emisions. Based on the study of Z. Wang & Calderon (2012), 0.33 tons CO_2 equivalent (CO_2eq) was emitted per ton of WH landfilled. So, the total CO_2eq emitted by the landfill was determined.

II.2.3.2. Scenario 2: Water hyacinth and banana peels to biohydrogen pathway

This approach deals with the conversion of WH and BP wastes to hydrogen by dark fermentation. For the comparison of the two scenarii, it was admitted that the quantity and the cost for the collection and transportation of WH and BP are the same in the two scenarii (Table 5). However, adding to the collection and transportation cost, the processing cost (pretreatment, labor, facilities, etc.) and the revenues earned from the selling of the fermentation products (H_2 and digestate) were considered for this scenario. This scenario was simulated using SPD.

The pretreatment was essentially the crushing of the feedstock. The buying price of the grinder was 3,700 USD (Alibaba.Com), and had a lifetime of 15 years. Its power was 15 kW with a capacity of 5 tons h^{-1}. The cost of electricity was 0.2 USD kWh^{-1}. So, the electricity consumed for grinding one ton of the feedstock cost 0.6 USD and the cost of the grinder for one ton of feedstock over its 15 years lifetime is 0.28 USD ton^{-1}. The overall cost of the pretreatment step is 0.88 USD ton^{-1} (Table 5). The other costs related to infrastructure, facilities, maintenance, labor, etc. are calculated by the algorithm of SPD. Additional costs related to materials imports, contingency, etc., were taken into account as additional costs in the simulation software (SPD). As previously stated, the biohydrogen plant would be located where a truck transportation of the feedstock consumes a maximum of four (04) liters of diesel to minimize transportation cost. The cost of hydrolase and inoculum purchase was not considered.

The selling prices of the products mainly hydrogen and the digestate were also estimated. The selling price adopted for hydrogen was 50 USD kg^{-1} (Randolph et al., 2017). The cost of the digestate was assumed to be 0.5 USD kg^{-1}. Table 6 summarizes the selling prices of the products.

For GHG emissions, as previously stated, the boundary of the life cycle analysis was considered from the production to the end-use of the products. It was assumed that the plant

was supplied with electricity from hydropower. So, emissions related to the plant energy consumption were neglected. The CO_2 emissions from the fermentation process were given by the simulation. The quantity of hydrogen produced was used to substitute coal in a cement industry. The low heating value of hydrogen is 120 MJ/kg while the heating value of coal is 24 MJ/kg (World Nuclear Association). So, one kg of H_2 could replace five kg of coal. Moreover, one kg of coal emits 2.86 kg of CO_2 (U.S. Energy Information Administration). Additionally, the production of one ton of organic fertilizer can avoid about 68.5 kg of CO_2 emissions to the atmosphere based on the nutrients content of the organic fertilizer (Z. Wang & Calderon, 2012). So, the amount of CO_2 to be reduced from the use of hydrogen and the organic fertilizer produced was determined and that quantity was sold on the carbon credit market to increase the project revenues. One ton of CO_2 cost 100 USD (UN Global Compact).

Table 5: Feedstock collection and pretreatment costs

Item	Cost (USD/ton)
Means for WH collection	2
Labor for WH collection	2
BP collection	0
Driver	1.6
Diesel	1.04
Pretreatment (crushing)	0.88
Total WH harvest, transportation, and pretreatment cost	7.52
Total BP transportation and pretreatment cost	3.52

Table 6: Products and their selling prices

Output	Selling Price (USD/kg)
Hydrogen	50
Digestate	0.5

For the simulation in SPD, three tons of feedstock (WH and BP) were considered per batch. The mass ratio of WH to BP was maintained at 70:30. So, per batch, 2.1 tons of WH, 0.9 tons of BP, and 10,000 L of water were supplied. The lifetime of the project was 15 years. The different steps considered for dark fermentation are summarized in Figure 8.

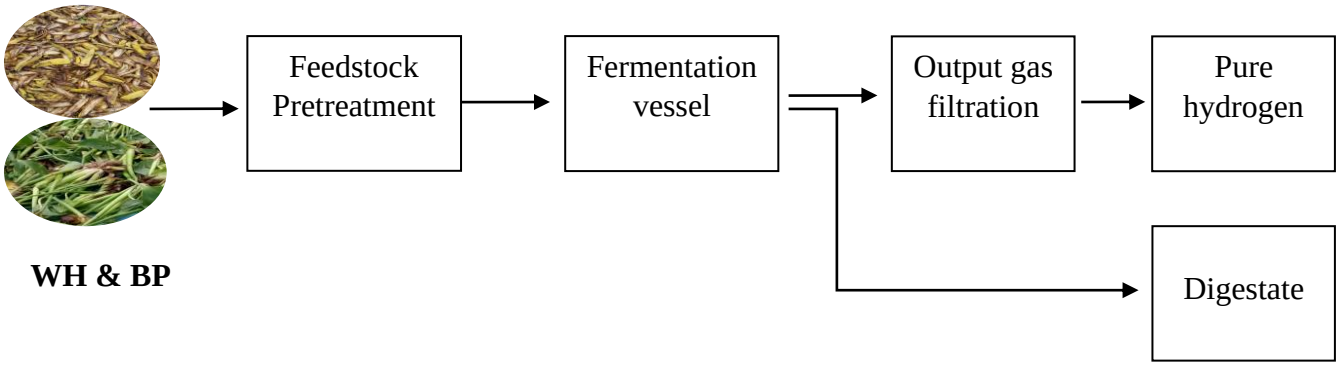

Figure 8: The different stages of dark fermentation

II.2.4. Biogas production test

II.2.4.1. The inoculum collection

The inoculum used for batch AD tests was fetched from an agricultural residues and cow manure mesophilic biogas plant in the locality of Rostock, Germany. The inoculum was fetched using a plastic bucket. The inoculum was kept untreated for the batch tests.

II.2.4.1. Batch anaerobic digestion tests of WHS, WHL, and BP

The batch AD tests were carried out following the VDI 4630 regulation. Fifteen glass flask bottles of a volume of 500 mL were rinsed to host the batch experiments. A magnetic stirring rod was introduced in all the flask bottles. The inoculum was stirred until homogeneity was achieved using a medium size stick. To ensure an adequate ratio between the inoculum and the substrates (around 0.4 F/M) in the fermentation medium, a constant mass of 200 g was adopted for the inoculum.

200 g of the homogenous inoculum was fed in the fifteen flask bottles using a funnel and a graduated cup. Then five grams of cellulose was similarly fed into three of the bottles, six grams of homogenous WHL was introduced in three other bottles, seven grams of homogenous WHS was fed into three other bottles, six grams of homogenous BP was fed into three other bottles, and the three remaining bottles were kept blank. Lastly, 100 g of tap water was added to all the flask bottles using a funnel and a graduated cup as well. Here, the cellulose and the blank bottles were considered as the digestion controls. The bottles were subsequently sealed with gas stoppers and electric modules for gas measurement connected to a computer to collect biogas generation data (Figure 9). All the bottles were then placed in a temperature-regulated water bath (Julabo TW20) set at a mesophilic temperature of 37^{o}C. The

bottles were stirred every day for one week, and then every two days for the remaining time (two weeks) using a magnetic stirrer. Figure 9 shows the main steps of the anaerobic digestion test setup.

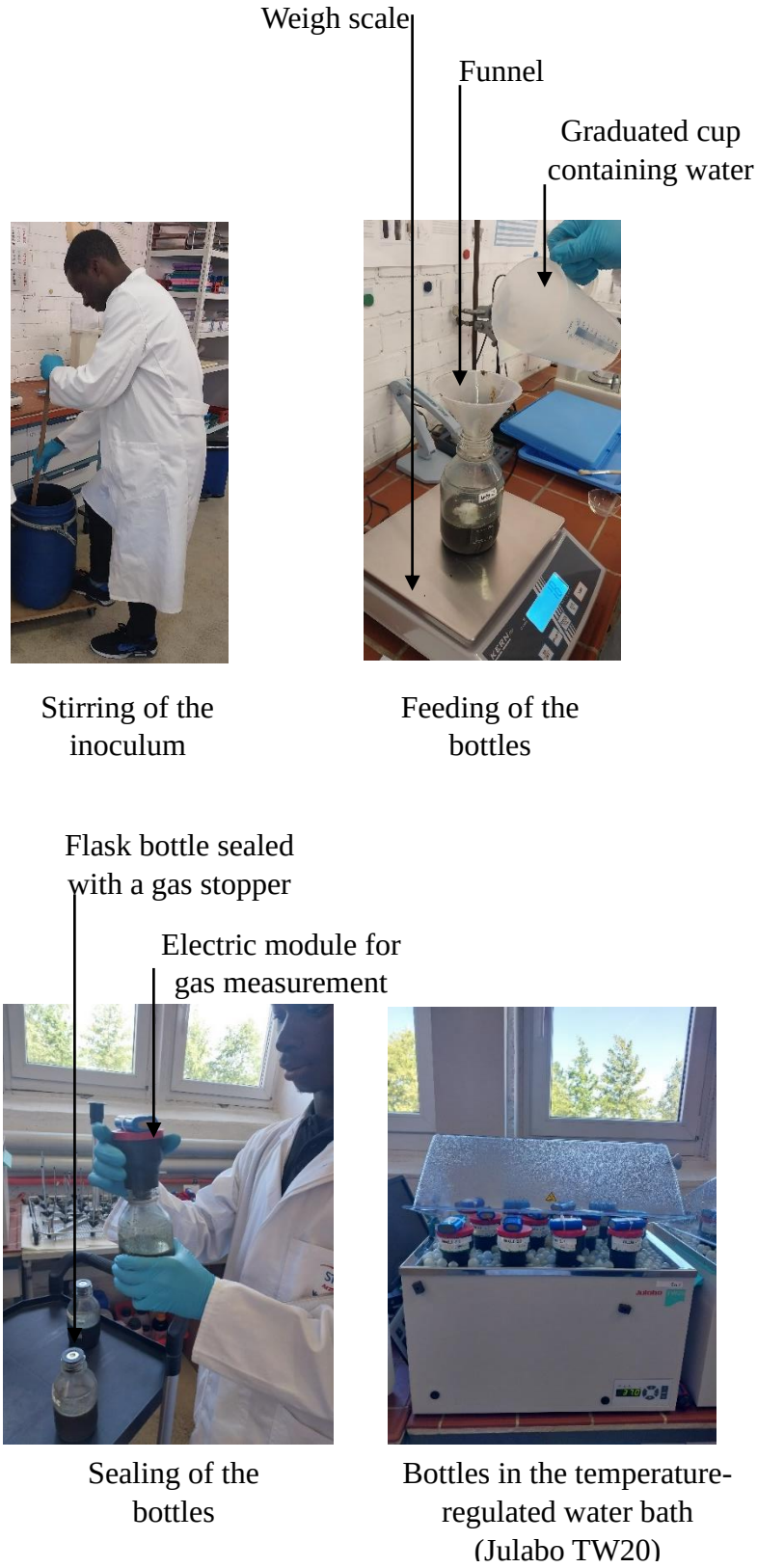

Figure 9: The different steps of the AD test of WHS, WHL, and BP samples

CHAPTER III: RESULTS AND DISCUSSION

III.1. Results

III.1.1. Characterization of water hyacinth and banana peel biomasses

III.1.1.1. Ultimate analysis

As shown in Figure 10, the elemental analysis revealed that the major chemical components of WHL are carbon (C) and oxygen (O) with respectively 30.58% and 29.76%. The detected hydrogen content in the leaves was 18%. The existence of certain minerals in WHL such us potassium (K), sodium (Na), and silicon (Si), was identified respectively in the proportions of 15.52%, 2.52%, and 3.54%. Moreover, calcium (Ca) and magnesium (Mg) were detected only once in the multi-points line measurement, so they were considered trace elements and were not included in the mean calculations.

The analysis of the stems showed a higher mass percentage of oxygen reaching up to about 48% (Figure 10). On the contrary to the composition of the leaves, silicon was not detected while the share of carbon, hydrogen, potassium, and sodium in the stems were respectively 28.7%, 8.8%, 10.74%, and 3.9%. It was remarked that hydrogen concentration in WHS was much lower compared with its concentration in WHL. Additionally, some minerals such as chlorine (Cl), calcium, and magnesium appeared in traces and were not treated in the data.

Similarly, the analysis of the roots revealed that oxygen content was about 47.62%. The lowest hydrogen and carbon concentration (4.9% and 18.44% respectively) were found in the roots (WHR) (Figure 10). A relatively high amount of potassium (22.32%) was identified while other minerals such as sodium, calcium, and silicon were detected in the proportions of 5.36%, 0.76%, and 0.6%. Moreover, phosphorous (P) and magnesium were detected as well but they appeared once in the measurement.

The analysis of the BP sample revealed that it was mainly composed of carbon, hydrogen, oxygen, potassium, and silicon (Figure 10). Carbon was found as the most abundant element with a mass concentration reaching the level of about 49%. Hydrogen concentration was 14.14% while the percentage of oxygen atoms was relatively low (12.22%). Potassium and silicon were the main minerals found in the proportions of 23.36%, and 1.30% respectively. Iodine was identified once in the series of measurements and was considered a trace element.

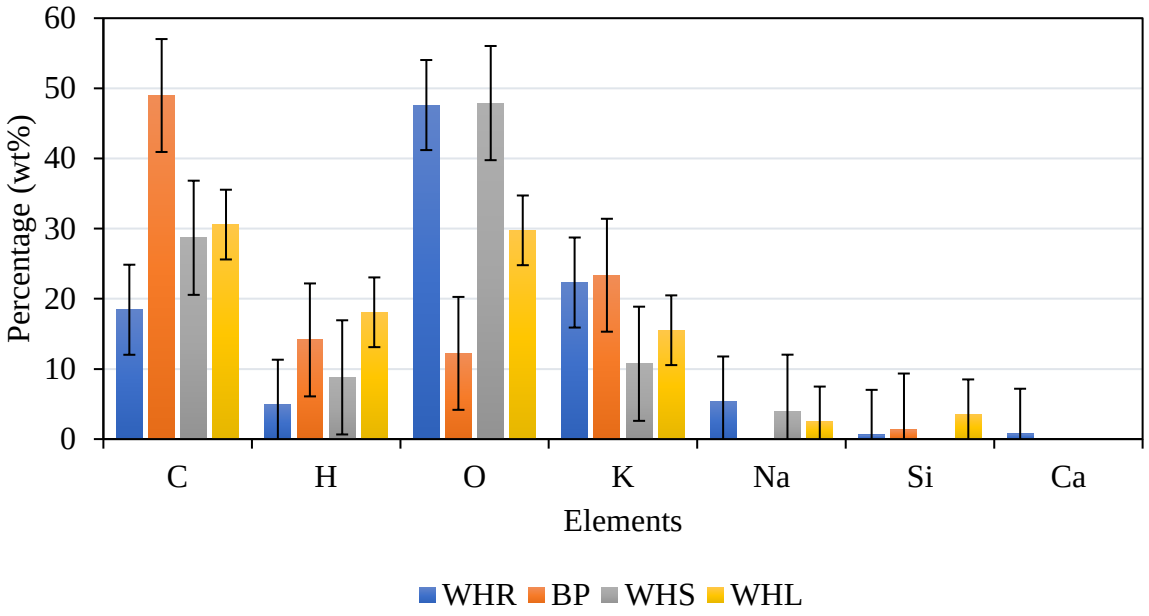

Figure 10: Elemental analysis of water hyacinth and banana peels

III.1.1.2. Proximate and fiber content analysis

The analysis of the fresh sample of WH revealed that it had over 94.16% of moisture and 5.84% of dry matter. Similarly, the analysis of the fresh sample of BP revealed a moisture content of 88.11% and a dry matter content of 11.89%. These results indicate that fresh WH contains more water as compared with BP waste. Moreover, the analysis of the mass distribution of WH plants showed that stems hold the highest share followed by the leaves as shown in Figure 11.

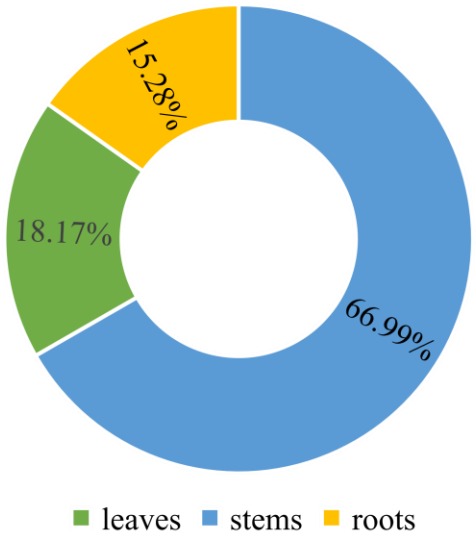

Figure 11: The mass distribution of water hyacinth (See Appendix E for the data)

The proximate analysis of the dried and ground samples of WH parts and BP is shown in Table 7. The results displayed the highest volatile solid content in BP (over 80.63%). The highest ash content was found in the roots and the stems (about 23%). WHL and BP contained a relatively low ash content which was only about 16%.

Table 7: Proximate analysis of water hyacinth parts and banana peels.

Parameter	WHL	WHS	WHR	BP
MC (wt%)	6.50±0.02	6.45±0.20	4.64±0.25	2.93±0.04
VS (wt%)	77.81±0.15	70.42±0.25	71.74±0.39	80.63±0.05
AC (wt%)	15.69±0.14	23.11±0.06	23.62±0.21	16.44±0.09
TS (wt%)	93.50±0.02	93.53±0.20	95.36±0.25	97.07±0.04

The fiber analysis revealed that WHS have the highest cellulose content (27.08%) while the lowest cellulose content (11.71%) was found in BP. It was also found that the highest lignin content (21.03%) was held by BP while the highest hemicellulose content (25.73%) was discovered in WHL. The detailed results of the fiber analysis can be found in Table 8.

Table 8: Fiber analysis of WH and BP samples

	BP	WHL	WHS	WHR
Cellulose (%TS)	11.71	18.73	27.08	21.22
Hemicellulose (%TS)	10.37	25.73	18.4	17.61
Lignin (%TS)	21.03	5.08	4.47	5.77

III.1.2. Hydrogen production rate and yield of the different mixing ratios between WH and BP

Figure 12 displays the cumulative hydrogen yield of the different mixing ratios from the simulation of dark co-fermentation of WH (leaves and stems) and BP using SPD. The results showed that the highest cumulative amount of hydrogen (over 124.64 mL g^{-1} VS) was generated from the mono-fermentation of WH (ratio 100:0). The co-fermentation of WH and BP at the ratio 70:30 yielded 110.52 mL g^{-1} VS while the ratio 50:50 generated about 99.85 mL g^{-1} VS after 24 h of HRT. The lowest hydrogen yield (67.36 mL g^{-1} VS) was recorded from the mono-fermentation of BP (ratio 0:100).

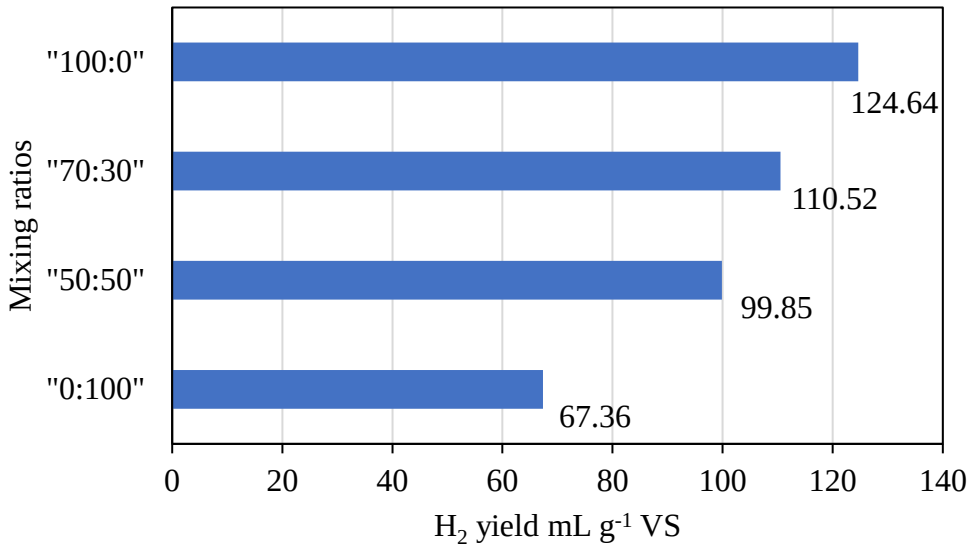

Figure 12: Hydrogen yield of the different mixing ratios (WH to BP)

On the other hand, the rate of hydrogen production, glucose consumption, bacterial growth, CO_2, and acetic acid formation were recorded. All the graphs showed similar behavior in the different ratios simulated.

As can be noticed in Figure 13, at the beginning of the kinetic fermentation, the concentration of glucose produced from the stoichiometric hydrolysis of cellulose in the medium is at its maximum value. The cell biomass which is the mixed culture bacteria provided by the inoculum is at its initial concentration whereas the products such as acetic acid, CO_2, and hydrogen are absent (0 g L^{-1}) at the start of the kinetic fermentation. As time was going on, glucose was being consumed by hydrogen-producing bacteria to grow while hydrogen and CO_2 were being released with the formation of acetic acid. Depending on the ratio, after some hours, glucose was completely consumed in the medium and the concentration of CO_2, acetic acid, and hydrogen became constant while the bacterial community reached its maximum growth (Figure 13, Figure 14, Figure 15, Figure 16)

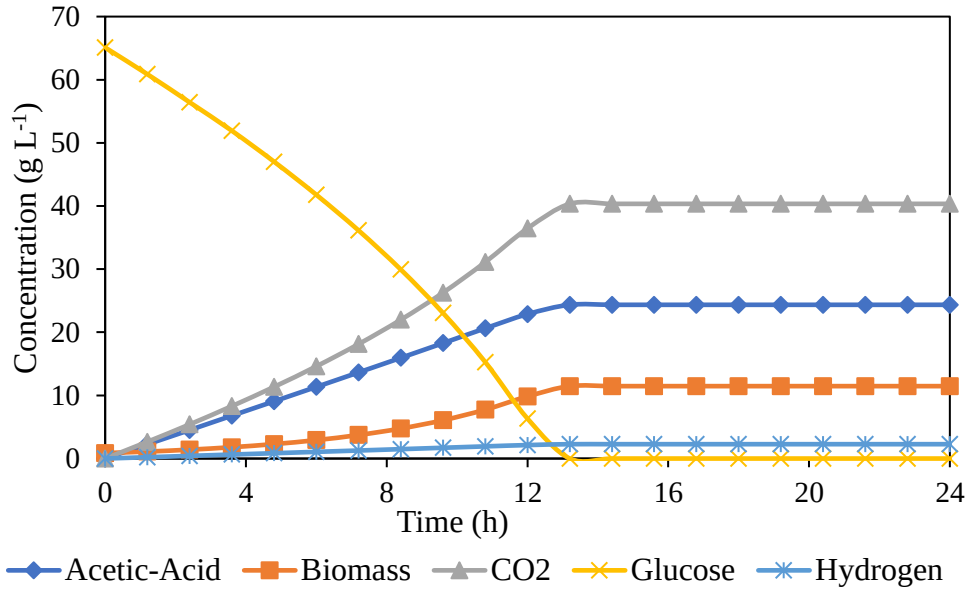

Figure 13: Simulated profiles of fermentation kinetics for the mixing ratio 100:0 (WH to BP)

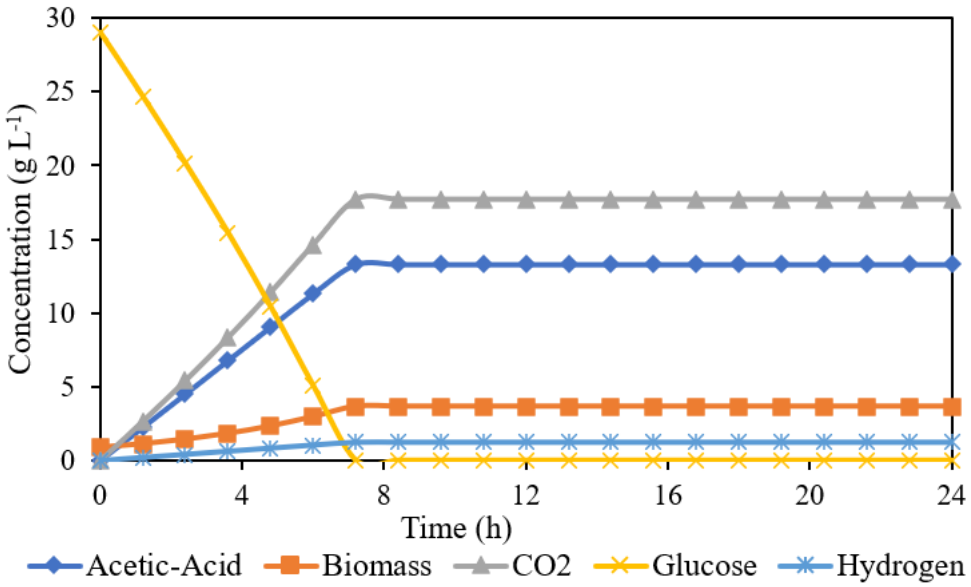

Figure 14: Simulated profiles of fermentation kinetics for the mixing ratio 0:100 (WH to BP)

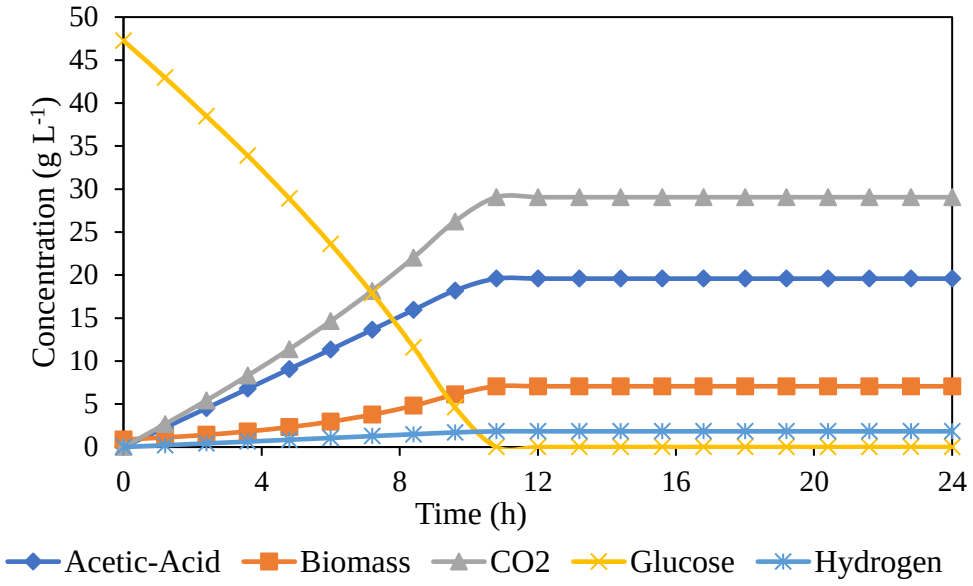

Figure 15: Simulated profiles of fermentation kinetics for the mixing ratio 50:50 (WH to BP)

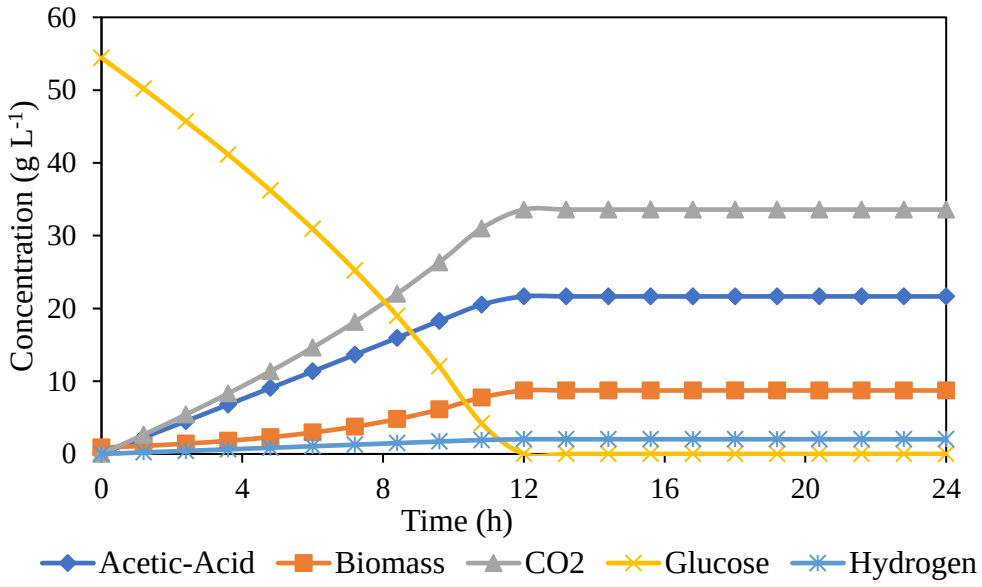

Figure 16: Simulated profiles of fermentation kinetics for the mixing ratio 70:30 (WH to BP)

The hydrogen production rates of the different substrate mixing ratios were plotted together in Figure 17. The figure shows that the highest hydrogen concentration was registered with the ratio WH to BP 100:0 reaching a maximum of 2.27 g L^{-1} after 13 h. The lowest H_2 concentration (a maximum of 1.24 g L^{-1} after 7 h) was registered with the ratio WH to BP 0:100. A maximum hydrogen concentration of 1.83 g L^{-1} (after 10 h) and 2.02 g L^{-1} (after 12 h) was registered respectively with the ratios WH to BP 50:50 and 70:30. In general, it was

observed that the hydrogen concentration increased quite linearly until the total consumption of glucose.

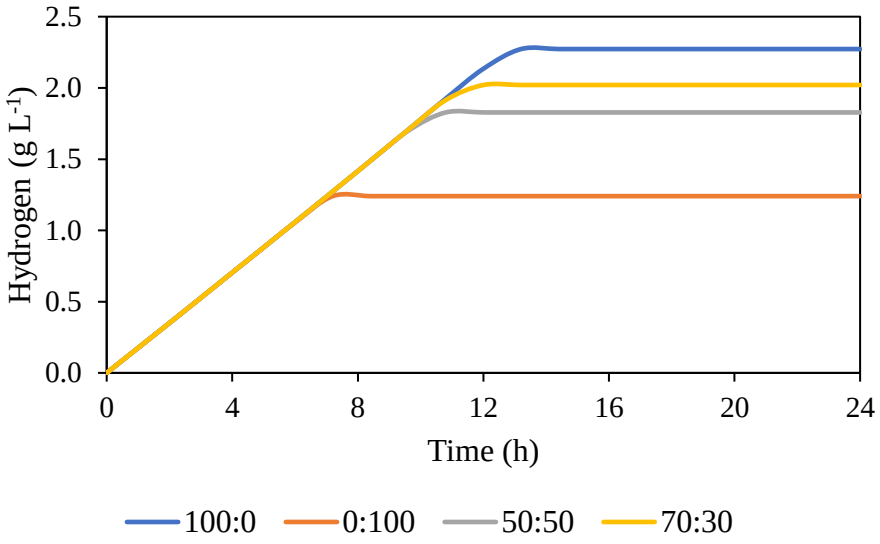

Figure 17: Hydrogen production rate of the different ratios

III.1.3. Economic and environmental analysis of the scenarios 1 and 2

III.1.3.1. Scenario 1

Scenario 1 consisted of harvesting WH and BP and transporting it straight to the landfill. The quantity of WH harvested in a year was calculated and the result was 616.37 tons (2162.7 kg × 285 batches). The total cost for harvesting and transporting WH was 4,092.70 USD yr^{-1} (616.37 tons × 6.64 USD ton^{-1}). Moreover, the quantity of BP collected in a year totaled 238.68 tons (837.47 kg × 285 batches). The total amount spent for BP transportation was 630.12 USD yr^{-1} (238.68 tons × 2.64 USD ton^{-1}). So, the overall total expenditure for the disposal of WH and BP wastes amounted to 4,722.82 USD yr^{-1} for a total of 855.05 tons yr^{-1} waste disposed of. Over 15 years lifetime, the total amount spent for WH and BP disposal into the landfill would be up to 70,842.3 USD.

The total CO_2eq emissions from the landfilling of WH and BP would be amounted to 282.17 tons yr^{-1} (0.33×855.05). over 15 years lifespan, this amount would be totaled to 4232.50 tons of CO_2 emitted to the atmosphere.

III.1.3.2. Scenario 2

In Scenario 2, WH and BP are collected and transformed into hydrogen and digestate. The results for the economic feasibility of the project simulated in SPD are shown in Table 9. As

in Scenario 1, the same quantity of WH and BP was collected in a year at the same cost (4,722.82 USD yr^{-1} for 855.05 tons yr^{-1}). The Payback Time obtained was 9.71 years

Table 9: Summary of the economic analysis of Scenario 2 without carbon credit (See Appendix F for the full report table)

CAPEX (USD)	OPEX (USD yr^{-1})	H_2 Revenue (USD yr^{-1})	Digestate Revenue (USD yr^{-1})	NPV (USD)
10,044,000	1,949,000	320,000	1,798,792	-2,353,000

The total quantity of CO_2 emitted from the fermentation process was 106.03 tons per year. The total hydrogen generated per batch was about 22.38 kg while the digestate left was around 12,623.11 kg. So, 6.38 tons of H_2 and 3,597.59 tons of fertilizer were generated yearly. The calculated amount of coal that could be replaced by the quantity of H_2 obtained was 31.9 tons (6.38×5). So, the use of the amount of H_2 produced in the cement industry which used coal would reduce about 91.23 tons (31.9×2.86) of CO_2 emissions yearly. The use of the organic fertilizer produced would reduce about 246.43 tons (3,597.59×0.0685) of CO_2 yearly. So, the total amount of CO_2 reduced by this scenario was 337.66 tons (91.23+246.43) per year. Balancing the CO_2 emissions from the fermentation process, the overall quantity of CO_2 that would be reduced by scenario 2 yearly was 231.63 tons (337.66-106.03).

The quantity of CO_2 reduced was sold on the carbon credit market and the revenues obtained amounted to 23,163 USD per year (231.63×100). The summary of the economic parameters taking into account the revenues from carbon credits is displayed in Table 10.

Table 10: Economic analysis of Scenario 2 with carbon credits

CAPEX (USD)	OPEX (USD yr^{-1})	H_2 Revenue (USD yr^{-1})	Digestate Revenue (USD yr^{-1})	NPV (USD)
10,044,000	1,949,000	329,000	1,823,975	-2,162,000

III.1.4. Biogas production rate and yield from water hyacinth leaves, stems, and banana peels

The results of the AD test on the samples of WHL, WHS, and BP were recorded and analyzed. The cumulative biogas production profile was recorded as shown in Figure 18. It was observed that biogas started being generated in all the bottles at different quantities right

after the experiment was set up. Then biogas production increased exponentially in the control bottle containing cellulose in the first week while a quite steady evolution was observed in the other control bottle (blank). In the same period, biogas yield increased quite steeply in the BP bottle while its increase in the WHS and WHL bottles was a bit lower but consistent. After the first week, biogas production enhancement slowed and became steady in all the bottles.

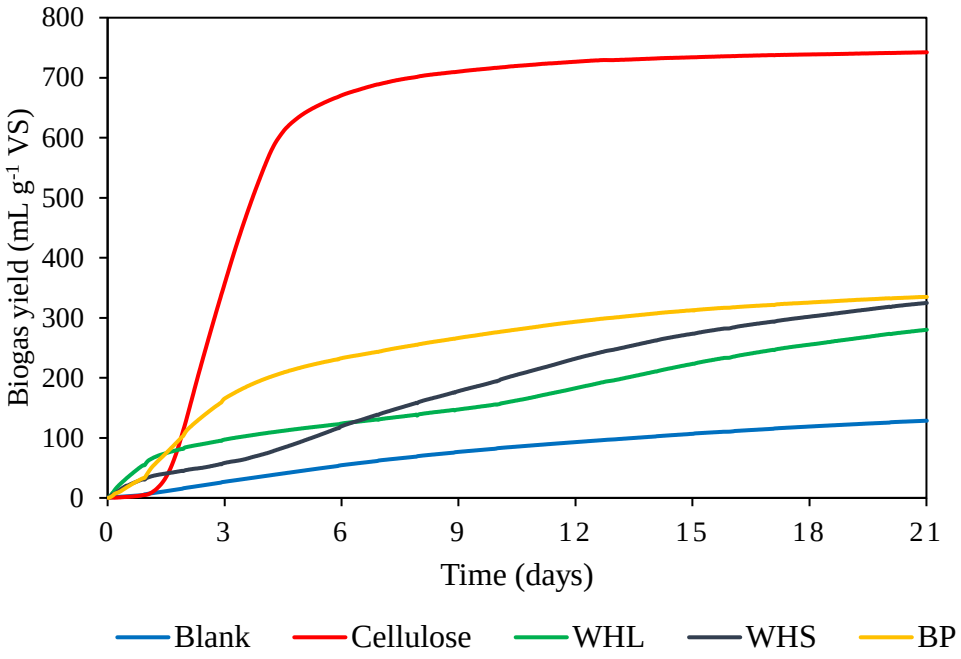

Figure 18: Cumulative biogas yield profiles

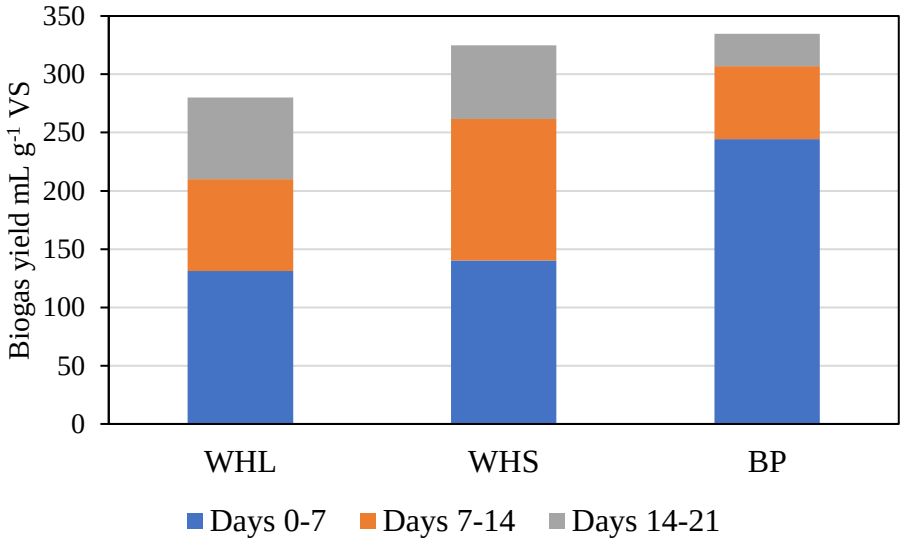

Figure 19: Weekly cumulative biogas yield from WHL, WHS, and BP

As observed in Figure 19, the net biogas yield from WHL, WHS, and BP in the first week was respectively 131.23, 140.18, and 244.23 mL g^{-1} VS. The degradation of BP was faster than the one of the other substrates. In the second week, WHS produced the highest biogas yield of 121.57 mL g^{-1} VS while WHL and BP produced respectively 78.84 mL g^{-1} VS and 62.88 mL g^{-1} VS. Three weeks later, on the 21st day, the experiments were stopped and the cumulative biogas yield registered for WHL, WHS, BP, cellulose, and blank samples were respectively 280.15, 324.79, 334.82, 742.27, and 128.58 mL g^{-1} VS as shown in Figure 18 and Figure 19.

III.2. Discussion

III.2.1. Chemical composition of water hyacinth and banana peels and its impact on biohydrogen production

As presented in Table 11, the standard error of most of the elements was relatively high. This is due to the multi-point line analysis of the samples (Figure 6). Some elements were not detected at some of the points, the value 0% was then assigned to those elements (Sukarni et al., 2019) and the mean was calculated based on five points analysis of each sample.

The results of the LIBS analysis of WH (Table 11) were comparable with the results obtained by Sukarni et al. (2019) from a similar analysis on WH. In the mentioned study, the mean and standard error were calculated based on four times analysis, and the results obtained in wt% were C (14.4±6.81), O (49.5±6.71), Na (0.58±0.40), Mg (1.96±1.04), Al (2.32±1.71), Zr (2.24±1.33), Cl (5.58±1.94), K (8.26±2.62), Ca (4.73±0.63), Si (5.33±4.52), Ti (0.27±0.27), Fe (4.71±4.32). The differences between these results and the results of the current study (Table 11) can be explained by many factors. In the current study, the LIBS analysis is done on separate parts of WH whereas in the previous study, it was done on WH as a whole plant. Moreover, the WH sample in the previous study originated from the shores of a dam in Indonesia while the samples of the current study are from a lake in the city of Lomé. So, it was deduced that the geographical location and the origin of WH could have an impact on its chemical composition. It can even be further deduced that the results of the current study could be more accurate as the mean values are computed from five points analysis of each sample.

On the other hand, the results of the elemental analysis of BP (Table 11) were confronted with the results obtained by Kabenge et al. (2018) on the characterization of BP waste. In the previous study, the measurement method was the ULTRA CHS-580 elemental analysis. The results obtained in wt% were as follow: C (35.4±0.21), H (6.19±0.07), N (1.94±0.16), O

(45.94±0.17), and S (20.75±9.55). The gaps between the results of the two studies can be explained by the divergence between the ULTRA CHS-580 elemental analysis and the LIBS analysis methods.

Table 11: Elemental composition of WH parts and BP

Chemical elements	Composition (wt%)			
	BP	WHL	WHS	WHR
C	48.98±4.62	30.58±9.51	28.70±2.17	18.44±5.53
H	14.14±1.55	18.08±7.28	8.80±0.46	4.90±2.05
O	12.22±7.72	29.76±12.28	47.90±1.91	47.62±2.07
K	23.36±4.18	15.52±5.64	10.74±0.84	22.32±5.71
Na	-	2.52±0.67	3.90±0.52	5.36±0.27
Ca	-	-	-	0.76±0.47
Si	1.30±0.84	3.54±2.41	-	0.60±0.39

As can be seen in Table 11, hydrogen content is not negligible in BP, WHL, and WHS. This showed how important is the potential for hydrogen production from these substrates. Conversely, the relatively high content of carbon and oxygen detected in the different samples as compared with hydrogen content, could constitute a source of carbon dioxide and fermentation by-products such as volatile fatty acids (VFAs) forming. The minerals found in the different biomasses (K, Na, Ca, Si, P, and Mg) can contribute to improving the cell growth and the formation of bioparticles (granular) inside the fermenter while increasing the hydrolytic capacity (Rajagopalan et al., 2014). In general, the presence of traces of minerals which are considered micro-nutrients could alleviate the nutritional requirements of the bacterial community in the fermentation medium. However, large amounts of minerals may lead to inhibitory effects on the fermentation process by involving into side-reactions.

Furthermore, digestion or fermentation processes have strict requirements for macro- and micro-nutrients for process stability. Macro-nutrients such as C, N, P, etc. contribute to the synthesis of carbohydrates, lipids, and proteins while micro-nutrients such as K, Ca, Mg, etc. behave as enzymes and co-factors in fermentation medium (Pérez-Rangel et al., 2020). The

poor content of hydrogen and the high amount of oxygen in WHR make it an inadequate substrate for fermentative hydrogen production.

III.2.2. Proximate and fiber content analysis of water hyacinth and banana peels: potential for biohydrogen production

III.2.2.1. Proximate analysis and its implications for the dark fermentation process

As shown in the results, freshly harvested WH and wet BP had high water content. The result for the moisture content of fresh WH (94.16%) is comparable with the result found by Omondi et al., (2019) which was 91%. The difference here can be related to the age of the harvested WH and its origin. As far as dark fermentation is concerned, the amount of moisture available in WH and BP makes them suitable to undergo fermentation. Dark fermentation requires a lot of water in the medium, so very wet substrates would be preferred to reduce the usage of drinkable water. Looking at the mass distribution of water hyacinth's parts, stems have the highest share (Figure 11). The relatively low mass share of the leaves and the roots could mean that discarding the roots from the feedstock for dark fermentation would not affect much the feedstock supply from WH.

The results of the proximate analysis of the dried WH parts (Table 7) compared closely with the results reported by Elsamadony & Tawfik (2018). In the previous work, the VS and the TS of WH as a whole plant were respectively on a dry basis 73.08% and 97.54%. Cheng et al. (2010) found similar results on ash content (AC) of WH parts. They found an ash content of 12.95%, 20.26%, and 49.97% for WHL, WHS, and WHR respectively. The differences between these results and the results found by the current study could be mainly due to the maturity of the samples and their origins. The current study used young WH plants before their flowering. The VS and AC of BP found in this study compared favorably with the study by Kabenge et al. (2018). They found that the VS and AC for BP are respectively 88.02% and 9.28%.

The high VS content (70 to 80%) shown by the different samples (BP, WHL, WHS) (Table 7) constitutes a valuable potential for biohydrogen production via dark fermentation Chen et al., 2022). The major part of the VS (fermentable VS) would degrade into fermentation products such as VFAs, hydrogen, and carbon dioxide. On the contrary, the relatively elevated AC in WHS and WHR (Table 7) can initiate process inhibition in the fermentation medium. As stated previously, the high concentration of minerals in the fermentation medium leads to an inhibition effect, and ash is mainly composed of minerals. Yi et al. (2014) reported that

increasing the total solid content (TS) of the feedstock in anaerobic digestion increases the bacterial community and methane yield. So, the high TS percentage shown in the different substrates (Table 7) is beneficial for bacterial growth and the product yield (H_2) in the fermentation process.

III.2.2.2. Fiber content and its contribution to biohydrogen production by dark fermentation

As shown in Figure 20, the results of the fiber content analysis of WH parts presented quite a wide disparity. The results shown in Table 8 were compared with the results registered by Cheng et al. (2010) who performed a similar analysis on WHL, WHS, and WHR. They found cellulose content to be in the range of 17-28.91%, hemicellulose content to be in the range of 15-30.80%, and lignin content to be in the range of 4-17.44% for WHR, WHS, and WHL respectively. Furthermore, the results of this study (Table 8) compared closely with the results reported by Omondi et al. (2019). In the mentioned study, the analysis was implemented on a whole WH biomass (leaves, stems, and roots together) and the results obtained were 9.9% of lignin, and 56% of holocellulose (cellulose + hemicellulose).

The gaps observed between the results of this study and the mentioned studies may be explained by the degree of maturity of the samples as well as their geographical location and origin. The degree of maturity can influence the rigidity of the plants; hence it influences their fiber composition. Moreover, the nature and concentration of available nutrients for plant growth may have an impact on the plant's physicochemical properties.

The composition of the fiber content found in the BP samples (Table 8) was confronted with the results obtained by Nathoa et al. (2014) who reported an 8.4% of cellulose portion, and 5.3% of hemicellulose portion in a wet BP sample. Moreover, Lara et al. (2020) found similar results which were 8.64% of cellulose, 14.16% of hemicellulose, and 9.26% of lignin portions in BP biomass.

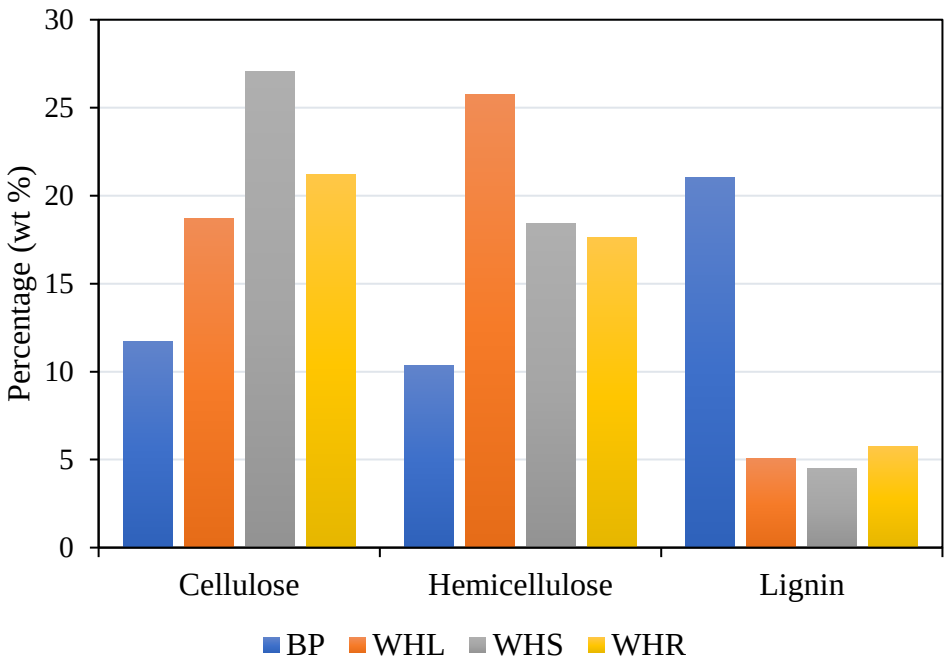

Figure 20: Fiber content of WH and BP (See Appendix F for the data table)

The content of cellulose and hemicellulose (Figure 20) in WHL, WHS, and WHR is consistent with the VS content found in those substrates. These important proportions of cellulose and hemicellulose represent considerable potential for biohydrogen production from WH and BP. In fact, in the dark fermentation process, hydrogen production is mainly derived from the degradation of cellulose and hemicellulose. In an anaerobic fermentation medium, cellulose hydrolyzes into glucose at a maximum efficiency of 90% with the impact of pre-treatment (Jiang et al., 2018). Consequently, a high content of cellulose implies an abundant availability of glucose for fermentation. Glucose is a preferred substrate for biohydrogen production given its relatively easy degradation and consumption by hydrogen-producing bacteria. Under specific conditions (141^{o}C), hemicellulose can hydrolyze to xylose up to 60% (Yuan et al., 2021). So, the major part of hemicellulose is converted to xylose which is a potential substrate for hydrogen production by dark fermentation in specific bacteria and heat requirements.

However, Lignin constitutes the main challenge in the hydrolysis step during dark fermentation. Lignin is rigid and it holds the matter against the release of cellulose and hemicellulose content into the fermentation process. High lignin content could delay the hydrolysis of cellulose and hemicellulose, lowering thus the hydrogen yield while extending the fermentation time. So, high lignin content could create inhibition in the fermentation

medium by stagnating the substrate hydrolysis. Consequently, the low lignin content observed in WHL, WHS, and WHR (Figure 20) may imply that those substrates degrade faster than BP in a dark fermentation medium.

III.2.3. Hydrogen production by dark fermentation of WH and BP: the effect of co-fermentation on hydrogen yield

The results in Figure 12 were compared with experimental results found in the literature about dark fermentation of WH and BP. The result of hydrogen yield (124.64 mL g^{-1} VS) from the ratio 100:0 was compared with the result registered by Elsamadony & Tawfik (2018). In the mentioned study, sodium chlorite was supplemented to the fermentation medium as a delignifying agent to achieve 119.9 mL (H_2) g^{-1} VS. The current results were further compared with the results obtained by Cheng et al., (2015). They found a hydrogen yield of 134.9 mL g^{-1} VS after hydrolyzing WH with activated carbon detoxification and bacteria domestication. The results of the ratio 0:100 (67.36 mL g^{-1} VS) compared closely with the findings of Ahmad et al. (2022) which were 78 mL (H_2) during the dark fermentation of BP. Moreover, regarding the co-fermentation of WH and BP, the results of the ratios 50:50 and 70:30 (99.85 mL g^{-1} VS and 110.52 mL g^{-1} VS respectively) were higher than the results registered by Yang & Wang (2019). In the previous study, they co-fermented sewage sludge and grass residue (ratio 3:7 VS), and found a hydrogen yield of 45.6 mL g^{-1} VS.

The differences observed between the simulation results of this study and the experimental results of the other studies as compared previously can be explained by several factors. This could be due to the fact that inhibition effects are ignored by the model used in SPD software whereas inhibition effects naturally influence hydrogen yield in the experimental cases. The gaps could also be due to the differences in the substrates' chemical compositions. Furthermore, the substrate concentration and the effect of microorganisms may influence the hydrogen yield.

The comparison of hydrogen yield from the different mixing ratios between WH and BP gave the highest yield (124.64 mL g^{-1} VS) to the ratio 100:0 (the mono-fermentation of WH) while the highest yield was expected from the co-fermentation ratios (70:30 or 50:50). Actually, this is due to the fact that the only source considered for hydrogen production in this empiric model is glucose obtained from the hydrolysis of cellulose. From the analysis of the substrates, the highest cellulose content was found in WHS while the lowest cellulose content was found in BP. So, the higher the quantity of WH in the medium, the higher the quantity of

cellulose, the higher the amount of glucose, and the higher the hydrogen yield. Based on these results, cellulose concentration was the predominant factor for hydrogen yield in dark fermentation. In a co-fermentation context, the substrate with higher cellulose content tended to determine the hydrogen yield.

However, in real cases (experimental cases), several compounds from WH and BP hydrolysis including proteins, lipids, xylose, other pentoses and hexoses can contribute to hydrogen production in dark fermentation. In that case, the highest hydrogen yield would be generated by co-fermentation as it creates a strong consortium of substrates and nutrients for hydrogen production. For instance, in specific fermentation conditions (high temperature and corresponding bacteria), xylose is degraded to generate hydrogen following Equation (28) (Cheng et al., 2010).

$$C_5H_{10}O_5 + H_2O \rightarrow 2CH_3COOH + CO_2 + 2H_2 \quad (28)$$

Moreover, inhibition effects may be involved in the fermentation medium in real cases, which are ignored in the simulation case. In such cases, the mono-fermentation of the substrates (ratios 100:0 and 0:100) would be the most exposed to inhibition effects because of eventual toxic components and unbalanced nutrients leading to reactor instability. This would have a negative impact on hydrogen yield. So, in real cases, the co-fermentation would be more favorable for higher hydrogen yield as it could help in dissolving toxic particles, complementing nutrients, and bringing equilibrium and stability in the reactor (Barua et al., 2019). The ratio 70:30 generated the second-highest hydrogen yield (110.52 mL g^{-1} VS) from the simulation. In a practical case, this ratio would be the most suitable to achieve the highest hydrogen yield from WH and BP given the higher content of cellulose in WH and the synergistic effect of nutrients that could evolve from the two substrates.

Additionally, it should be noted that the model used by SPD to perform the simulations in this study proved some limits. The model could not take into account the effects of some intrinsic parameters such as pH. The pH of the fermentation medium plays an important role in hydrogen productivity. Furthermore, the contribution of inorganic nutrients could also not be simulated with this model which may have an impact on hydrogen yield. More understanding of reaction conditions and kinetics is needed to simulate the fermentation of other monomers such as xylose, maltose, saccharose, galactose, etc., and optimize hydrogen production.

III.2.4. Economic and environmental feasibility of fermentative hydrogen production from WH and BP in Lomé

To economically analyze and compare the landfill and biohydrogen scenarios, the economic benefits were assessed by comparing the disposals of WH and BP between the landfill scenario and the biohydrogen scenario. The comparison was based on the assumption that the same quantity of WH and BP (855.05 tons yr^{-1}) was disposed of in the two scenarios at the same cost (4,722.82 USD yr^{-1}). The considered project lifetime was 15 years. The annual working hours were 7915 hours (330 days).

In the landfill scenario, over 4,722.82 USD would be spent every year for the disposal of WH and BP wastes, which constitutes an important economic loss. Additionally, the landfill would emit about 282.17 tons CO_2eq per year into the atmosphere which jeopardizes efforts toward reducing greenhouse gas (GHG) emissions. The only benefits could be the liberation of the water body of the lake which favors the practicing of fishing activities, navigation and recreation activities, as well as irrigation activities. Moreover, this scenario creates some jobs and livelihoods for people (e.g., labor for harvesting and transportation). In conclusion, scenario 1 is economically and environmentally not viable.

In the biohydrogen scenario, the benefits were assessed from the investment into the pilot plant and the revenues from the selling of products (hydrogen and the digestate) and carbon credits of CO_2 reduction over the project's lifespan. In the first place, the simulated NPV without carbon credits revenues was negative showing that instead of making profit, a loss of 2,353,000 USD would be generated over the project's lifetime. The NPV found for this scenario was compared with the NPV obtained by Bergman, (2016) in his study of hydrogen production from potato peels by dark fermentation using SPD. In the mentioned study, the simulated value of NPV was -96, 169, 000 USD assuming that no stream was recirculated as the case of this study. In the second place, the simulated NPV including carbon credits revenues was -2,162,000 USD showing that a loss would still occur over the project lifetime but much less than the one without carbon credits. Given the negative NPVs found for the project of scenario 2 (with and without carbon credits revenues), it should be concluded that scenario 2 is not economically viable as well. However, On the environmental aspect, this scenario does not emit GHGs into the atmosphere and even contribute to reducing over 231.63 tons CO_2eq every year. So, environmentally, Scenario 2 is sustainable. In addition, Scenario 2 creates several co-benefits. As in Scenario 1, it clears WH from the lake enabling the flow of economic activities, creating more jobs and livelihoods for people along the

transformation chain (e.g., job positions in the plant, indirect jobs, etc.). Furthermore, the digestate which constitutes an organic fertilizer after composting, would contribute to soil improvement and crop yield while reducing the use of chemical fertilizers.

In comparison of the two scenarios, Scenario 1 would generate expenditure up to 70,842.3 USD for WH and BP waste disposal while ejecting over 4,232.55 tons of CO_2eq into the atmosphere over the 15 years lifespan of the project. Meanwhile, Scenario 2 would generate a loss of about -2,162,000 USD including carbon credits while reducing up to 3,474.45 tons CO_2eq over the project's lifetime. In conclusion, Scenario 2 is the most sustainable and should be promoted over Scenario 1.

In this regard, although Scenario 2 is found to be not viable economically, with regards to its number of co-benefits and especially considering its improvement and optimization perspectives, it should be promoted over Scenario 1. To optimize the project of Scenario 2 and render it economically viable, an integrated system should be explored in which after dark fermentation step in the fermenter, the digestate which is rich in organic acids, is further converted into biogas by anaerobic digestion, then the final digestate from the reactor is composted with additional residues to produce organic fertilizer as designed in Figure 21. As reported by Judith Martínez et al. (2019), coupling dark fermentation with an alternative biological route such as AD would increase substrate conversion efficiency by promoting its efficient stabilization and use.

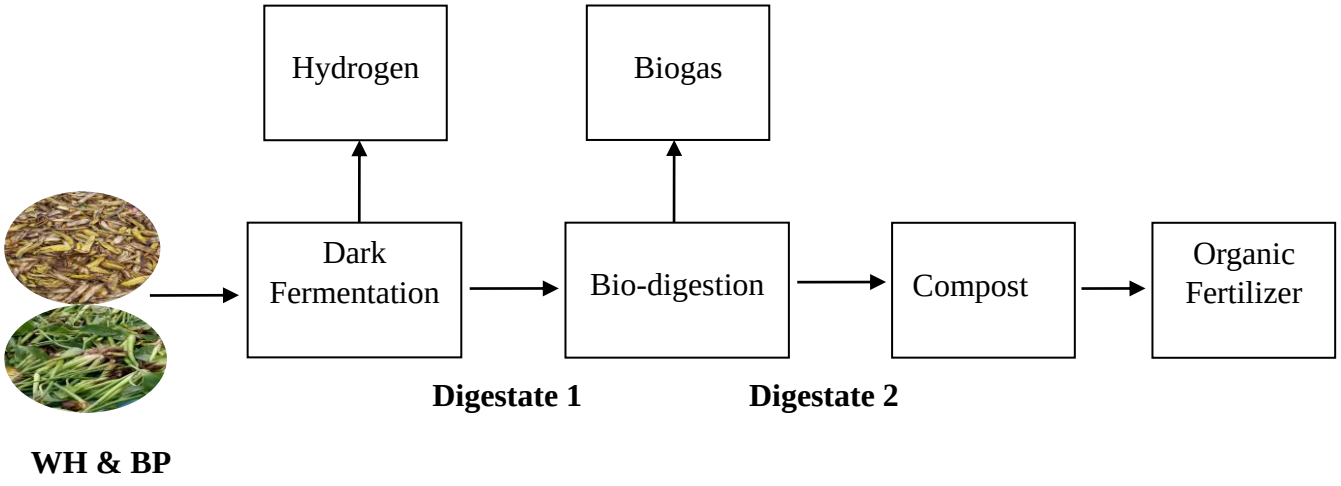

Figure 21: Optimization diagram for WH and BP conversion into biohydrogen (Scenario 2)

III.2.5. Anaerobic digestion of WH and BP: biogas potential

As observed in Figure 18, the exponential increase in biogas yield of the cellulose sample could mean that there was a sufficient availability of nutrients for bacteria in the anaerobic medium. The available nutrients were easily accessible by the consortium of bacteria which degraded them quite fast to produce biogas. In the blank sample, biogas production was lower and steady because of the lack of nutrients for microorganisms' activity. Biogas production from BP was higher than biogas production from WHL and WHS. This could be due to the fact that BP had the highest VS content (80.63%). The VS (fermentable VS) content is the source of biogas production in anaerobic digestion as it mostly incorporates a wide range of nutrients. The cellulose content of WHS (27.08%) was higher than the one of WHL (18.73%), and this had impacted biogas production from the two substrates as biogas yield from WHS increased slightly higher than the increase in biogas yield from WHL over the weeks. As observed in Figure 19, after the first week, the weekly cumulative biogas production decreased significantly as the available nutrients in the respective samples tended to be consumed up.

In conclusion, it should be noted that nutrient content of substrates is key to biogas production. For the different substrates, the VS and the cellulose content were determinant for biogas yield.

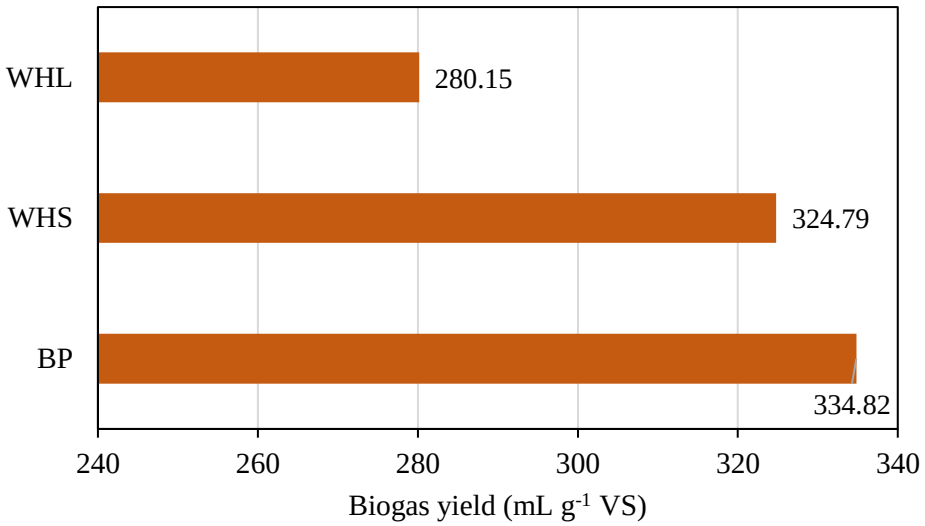

Figure 22: Cumulative biogas yield over 21 days HRT

The net cumulative values of biogas yield from WHS, WHL, and BP (Figure 22) were confronted with previous results found in the literature. The cumulative biogas yields found

for WHL and WHS were much higher than the results reported by Nugraha et al. (2018) in their study on biogas production from WH. They recorded a maximum of 151.91 mL g^{-1} VS at an optimum F/M ratio of 10.01 over an HRT of 160 days. Moreover, the biogas yield from the BP sample was compared closely with the results obtained by Achinas et al. (2019). In the mentioned study, it was reported a maximum biogas yield of 112.18 mL g^{-1} VS from the batch anaerobic digestion of BP at the concentration of 10 g VS L^{-1} with 10% cow manure as inoculum. The registered biogas yield from BP was further confronted with the findings of Odedina et al. (2017). They observed methane yield to be 330.6 mL g^{-1} VS and 268.3 mL g^{-1} VS respectively from ground and chopped BP. In the mentioned study, biogas yield was higher than the current results as the methane yield was between 50-60% of the total biogas yield.

The observed differences in the value of biogas yield recorded between the current study and the mentioned studies can be related to the substrate condition (wet or dry), the type of pretreatment applied on the substrate, the HRT, and the frequency of stirring. In fact, for lignocellulosic substrates such as WH and BP, pretreatment is key to ensure an optimum operation in the different steps of AD (hydrolysis, acidogenesis, acetogenesis, and methanogenesis) that leads to an optimum biogas yield. The condition and the nature of the substrate determine the type of pretreatment to apply. In this regard, Sarto et al. (2019) explained that pretreating WH before AD is an effective solution for improving its biodegradability. They further highlighted that pre-treatment breaks down cellulose and hemicellulose into readily biodegradable components while removing lignin from hemicellulose and cellulose clusters to make them accessible to micro-organisms. In this belief, Gao et al. (2013) experimented biogas production from pretreated WH at different temperatures and durations such as 100^{o}C for 120 min, 120^{o}C for 60min, and 120^{o}C for 120 min. They discovered that the highest biogas yield (170 mL g^{-1} VS) was registered from the WH pretreated at the highest temperature and for the longest time (120^{o}C for 120 min). In conclusion, the results from the current study can be further enhanced by applying chemical pretreatment to the already thermally and physically pretreated samples.

Moreover, HRT, the temperature, and the frequency of stirring have a strong correlation with biogas yield from AD. It should be remembered that for this study, the HRT was 21 days, and the bottles at a mesophilic temperature of 37-38^{o}C, were stirred every day in the first week and every two days subsequently using a magnetic stirrer. This had strongly influenced the current results. The 21 days HRT were sufficient to ensure the growth of bacteria responsible

for biogas production with respect to the nutrients available as the daily biogas production was getting lower towards the 21st day. The mesophilic temperature created a favorable environment for bacterial development and its optimum activity.

WHL, WHS, and BP are suitable substrates for biogas production by AD given their relatively high biogas productivity. The potential for biogas production from WH and BP is enormous. These resources should be harnessed to produce sustainable energy while eradicating their environmental drawbacks. So, it is necessary to scale up biogas production by ensuring the availability of the feedstock (WH and BP). As proposed previously, it could be coupled the production of hydrogen with the production of biogas from WH and BP in two-phase anaerobic digestion to optimize biohydrogen production chain while increasing the economic rentability of the project.

SUMMARY OF KEY FINDINGS, CONCLUSION, AND RECOMMENDATIONS

1. Summary

WH's invasion of the lakes in Lomé causes serious environmental and socio-economic drawbacks. This study attempted to propose a sustainable pathway to valorize WH and BP resources into hydrogen. WH and BP samples were characterized and the analysis revealed that freshly harvested WH plants had about 94.16% moisture while wet banana peels had 88.11% water content. The analysis of dried WH showed that the leaves, stems and roots represented respectively 18.17, 66.99, and 15.28%. Dried and ground WHL, WHS, WHR, and BP had respectively 77.81, 70.42, 71.74, and 80.63% VS content. The elemental analysis of the samples revealed that C, O, H, and K were the main components of WHL, WHS, WHR, and BP with a hydrogen share of respectively 18, 8.8, 4.9, and 14.14%. Chemical elements such as Na, P, Mg, and Si were found as traces in most of the substrates. The cellulose content in WHL, WHS, WHR, and BP was found to be respectively 18.73, 27.08, 21.22, and 11.71%.

The results of the characterization were used to simulate the co-fermentation of WH (stems and leaves) and BP using SPD. The results for the mixing ratios 100:0, 0:100, 50:50, and 70:30 was respectively 124.64, 67.36, 99.85, and 110.52 mL g^{-1} VS hydrogen yield. These results showed that cellulose was the predominant factor for hydrogen yield in dark co-fermentation as the substrate with the highest cellulose content tended to determine the hydrogen yield. The economic feasibility investigated between the scenarios of WH and BP waste into the landfill on one hand and biohydrogen on the other hand concluded that none of the scenarios was economically viable even with the inclusion of carbon credits revenues for the biohydrogen scenario. Scenario 1 (WH and BP into landfill) was not environmentally sustainable as it would eject about 282.17 tons CO_2eq into the atmosphere yearly. Meanwhile, Scenario 2 (WH and BP into landfill) was environmentally sustainable with an overall yearly CO_2 reduction of over 231.63 tons.

However, Scenario 2 (WH and BP to biohydrogen) was promoted with the perspective of integrating biogas production and composting units into the dark fermentation chain. An anaerobic digestion test of WHL, WHS, and BP was carried out. The results confirmed the adequacy of integrating AD into the dark fermentation process as the biogas yield of WHL, WHS, and BP samples reached respectively 280.15, 324.79, and 334.82 mL g^{-1} VS.

Some limitations were encountered. The simulation could not take into account the effect of pH and inhibition factors in the fermentation medium. Moreover, the contribution of micronutrients such as inorganic compounds could not be simulated. For the economic analysis, the storage of hydrogen was not included. Moreover, the scope for the emission-based life cycle analysis was considered from the production to the end-use of the products for Scenario 2 and from the landfilling of the biomasses to the GHG emissions for Scenario 1. In addition, the biogas produced could not be analyzed.

2. Conclusion and perspectives

Water hyacinth, the world's worst aquatic plant could become one of the most researched resources for biohydrogen production given its suitable chemical composition and characteristics for hydrogen production. In the context of energy insecurity, fossil fuel depletion and GHG emissions, climate change, and circular economy, WH and BP wastes in Lomé can be harnessed to produce sustainable fuels for electricity generation, transportation, machinery, and clean cooking. Green hydrogen production from WH and BP in Lomé can be rendered feasible and attractive by aligning together dark fermentation, anaerobic digestion, and composting in the same process to increase the project's efficiency and rentability.

This study has contributed knowledge on the fermentative hydrogen production from lignocellulosic biomass, specifically water hyacinth and banana peels. This helps to address the current gap of research in this particular area and provide real-world value to biohydrogen production. The study will serve as a guide to decision makers, for the sustainable valorization of water hyacinth and banana peels into biofuels in the city of Lomé and even beyond. This will thus reduce greenhouse gas emissions from improper waste management from banana and water hyacinth plants while contributing to the achievement of the United Nations Sustainable Development Goals (UN SDGs) especially the goals 7 (Affordable and clean energy), 13 (Climate action), and 14 (Life below water).

Future research in this particular area should focus on:

- Life cycle assessment of dark co-fermentation of WH and BP for hydrogen and biogas production
- Further research on the co-generation of hydrogen and methane from two-phase dark co-fermentation of WH and BP
- Dynamic modeling of dark fermentation processes.

3. Recommendations

For the implementation of this study and further research on this topic, this research work recommends:

- To the agencies and institutions in charge of WH management in Lomé and Togo at large, to collect data on WH availability throughout the year, the methods for harvesting, and the expenses generated by WH harvesting and its transportation
- The design of a business model for a sustainable valorization of WH into biogas and/or biohydrogen coupled with composting in Lomé

REFERENCES

Achinas, S., Krooneman, J., & Euverink, G. J. W. (2019). Enhanced Biogas Production from the Anaerobic Batch Treatment of Banana Peels. *Engineering*, *5*(5), 970–978. https://doi.org/10.1016/j.eng.2018.11.036

Ahmad, S. A. R., Singh, M., & Tiwari, A. (2022). Production of Bio-Hydrogen from Banana Waste by Using Anaerobic Fermentation. *International Journal for Research in Applied Science and Engineering Technology*, *10*(3), 1202–1205. https://doi.org/10.22214/ijraset.2022.40831

Aleixandre-Tudó, J. L., Castelló-Cogollos, L., Aleixandre, J. L., & Aleixandre-Benavent, R. (2019). Renewable energies: Worldwide trends in research, funding and international collaboration. *Renewable Energy*, *139*, 268–278. https://doi.org/10.1016/j.renene.2019.02.079

Alibaba.com. (n.d.). Retrieved June 3, 2023, from https://www.alibaba.com/showroom/grinder-machine-for-biomass.html

Argun, H., & Onaran, G. (2017). Effects of N/C, P/C and Fe/C ratios on dark fermentative hydrogen gas production from waste paper towel hydrolysate. *International Journal of Hydrogen Energy*, *42*(22), 14990–15001. https://doi.org/10.1016/J.IJHYDENE.2017.04.289

Barua, V. B. (2018). *Anaerobic Digestion of Water Hyacinth: Effect of Pretreatment and Co-Digestion on Biogas Production*. Doctoral thesis, Indian Institute of Technology Guwahati, India, 20-200.

Barua, V. B., Rathore, V., & Kalamdhad, A. S. (2019). Anaerobic co-digestion of water hyacinth and banana peels with and without thermal pretreatment. *Renewable Energy*, *134*, 103–112. https://doi.org/10.1016/j.renene.2018.11.018

Bergman, E. (2016). *Evaluation of the software SuperPro Designer through simulation of a biohydrogen production process*. Master thesis, Lund University, Sweden.

Carosia, M. F., dos Reis, C. M., Sakamoto, I. K., Varesche, M. B. A., & Silva, E. L. (2017). Influence of C/P and C/N ratios and microbial characterization in hydrogen and ethanol production in an anaerobic fluidized bed reactor. *International Journal of Hydrogen Energy*, *42*(15), 9600–9610. https://doi.org/10.1016/J.IJHYDENE.2017.01.127

Chandrasekhar, K., Lee, Y. J., & Lee, D. W. (2015). Biohydrogen production: strategies to improve process efficiency through microbial routes. *International Journal of Molecular Sciences*, *16*(4), 8266–8293. https://doi.org/10.3390/IJMS16048266

Chen, H., Wu, J., Huang, R., Zhang, W., He, W., Deng, Z., Han, Y., Xiao, B., Luo, H., & Qu, W. (2022). Effects of temperature and total solid content on biohydrogen production from dark fermentation of rice straw: Performance and microbial community characteristics. *Chemosphere*, *286*, 131655. https://doi.org/10.1016/J.CHEMOSPHERE.2021.131655

Cheng, J., Lin, R., Song, W., Xia, A., Zhou, J., & Cen, K. (2015). Enhancement of fermentative hydrogen production from hydrolyzed water hyacinth with activated carbon detoxification and bacteria domestication. *International Journal of Hydrogen Energy*, *40*(6), 2545–2551. https://doi.org/10.1016/j.ijhydene.2014.12.097

Cheng, J., Xie, B., Zhou, J., Song, W., & Cen, K. (2010). Cogeneration of H2 and CH4 from water hyacinth by two-step anaerobic fermentation. *International Journal of Hydrogen Energy*, *35*(7), 3029–3035. https://doi.org/10.1016/j.ijhydene.2009.07.012

Colbertaldo, P., Agustin, S. B., Campanari, S., & Brouwer, J. (2019). Impact of hydrogen energy storage on California electric power system: Towards 100% renewable electricity. *International Journal of Hydrogen Energy*, *44*(19), 9558–9576. https://doi.org/10.1016/J.IJHYDENE.2018.11.062

Elsamadony, M., & Tawfik, A. (2018). Maximization of hydrogen fermentative process from delignified water hyacinth using sodium chlorite. *Energy Conversion and Management*, *157*, 257–265. https://doi.org/10.1016/j.enconman.2017.12.013

Gao, J., Chen, L., Yan, Z., & Wang, L. (2013). Effect of ionic liquid pretreatment on the composition, structure and biogas production of water hyacinth (Eichhornia crassipes). *Bioresource Technology*, *132*, 361–364. https://doi.org/10.1016/j.biortech.2012.10.136

Haque, S., Singh, R., Pal, D. B., Faidah, H., Ashgar, S. S., Areeshi, M. Y., Almalki, A. H., Verma, B., Srivastava, N., & Gupta, V. K. (2022). Thermophilic biohydrogen production strategy using agro industrial wastes: Current update, challenges, and sustainable solutions. *Chemosphere*, *307*, 136120. https://doi.org/10.1016/J.CHEMOSPHERE.2022.136120

Hasibar, B., Ergal, İ., Moser, S., Bochmann, G., Rittmann, S. K. M. R., & Fuchs, W. (2020). Increasing biohydrogen production with the use of a co-culture inside a microbial electrolysis cell. *Biochemical Engineering Journal*, *164*. https://doi.org/10.1016/j.bej.2020.107802

Hudakorn, T., & Sritrakul, N. (2020). Biogas and biomass pellet production from water hyacinth. *Energy Reports*, *6*, 532–538. https://doi.org/10.1016/j.egyr.2019.11.115

Intelligen, Inc. (n.d.). Retrieved May 27, 2023, from https://www.intelligen.com/products/superpro-overview/

Jain, R., Panwar, N. L., Jain, S. K., Gupta, T., Agarwal, C., & Meena, S. S. (2022). Bio-hydrogen production through dark fermentation: an overview. In *Biomass Conversion and Biorefinery*. Springer Science and Business Media Deutschland GmbH. https://doi.org/10.1007/s13399-022-03282-7

Jan Liebetrau, E., & Pfeiffer, D. (2020). *Biomass energy use Collection of Methods for Biogas*. Report, DBFZ, Germany, 50-106.

Jayachandran, V., & Basak, N. (2023). Optimization of dark fermentative biohydrogen production from rice starch by Enterobacter aerogenes MTCC 2822 and Clostridium acetobutylicum MTCC 11274. *Bioprocess and Biosystems Engineering*, *46*(4), 535–553. https://doi.org/10.1007/s00449-022-02838-1

Jiang, H., Cao, Z., Gonzalez-Ortega, O., Lavoie, J.-M., Chang, K.-W. J., Kong-Win Chang, J., Duret, X., Berberi, V., & Zahedi-Niaki, H. (2018). Two-Step Thermochemical Cellulose Hydrolysis With Partial Neutralization for Glucose Production. *Front. Chem*, *6*, 117. https://doi.org/10.3389/fchem.2018.00117

Judith Martínez, E., Blanco, D., & Gómez, X. (2019). *Two-Stage Process to Enhance Bio-hydrogen Production* (pp. 149–179). https://doi.org/10.1007/978-3-030-10516-7_7

Kabenge, I., Omulo, G., Banadda, N., Seay, J., Zziwa, A., & Kiggundu, N. (2018). Characterization of Banana Peels Wastes as Potential Slow Pyrolysis Feedstock. *Journal of Sustainable Development*, *11*(2), 14. https://doi.org/10.5539/jsd.v11n2p14

Kim, S. H., Kumar, G., Chen, W. H., & Khanal, S. K. (2021). Renewable hydrogen production from biomass and wastes (ReBioH2-2020). *Bioresource Technology*, *331*, 125024. https://doi.org/10.1016/J.BIORTECH.2021.125024

Koók, L., Szabó, Á., Bakonyi, P., Tóth, G., Bélafi-Bakó, K., & Nemestóthy, N. (2014). Process simulation of integrated biohydrogen production: hydrogen recovery by membrane separation. In *Journal of Agricultural Informatics* (Vol. 5, Issue 2). http://www.magisz.org/journal

Kothari, R., Kumar, V., Pathak, V. V, Ahmad, S., Aoyi, O., & Tyagi, V. V. (2017). A critical review on factors influencing fermentative hydrogen production. In *Frontiers In Bioscience* (Vol. 22).

Kumar, G., Sivagurunathan, P., Pugazhendhi, A., Thi, N. B. D., Zhen, G., Chandrasekhar, K., & Kadier, A. (2017). A comprehensive overview on light independent fermentative hydrogen production from wastewater feedstock and possible integrative options. *Energy Conversion and Management*, *141*, 390–402. https://doi.org/10.1016/J.ENCONMAN.2016.09.087

Lara, M. A., Méndez, E. F., Malagón, D. H., Bernal, J. M., & Montoya, D. (2020). Evaluation of production of hydrogen in a batch bioreactor using Clostridium butyricum DSM 2478 from banana peel. *Chemical Engineering Transactions*, *79*, 265–270. https://doi.org/10.3303/CET2079045

Li, X., Guo, L., Liu, Y., Wang, Y., She, Z., Gao, M., & Zhao, Y. (2020). Effect of salinity and pH on dark fermentation with thermophilic bacteria pretreated swine wastewater. *Journal of Environmental Management*, *271*, 111023. https://doi.org/10.1016/J.JENVMAN.2020.111023

Li, Y., Alaimo, C. P., Kim, M., Kado, N. Y., Peppers, J., Xue, J., Wan, C., Green, P. G., Zhang, R., Jenkins, B. M., Vogel, C. F. A., Wuertz, S., Young, T. M., & Kleeman, M. J. (2019). Composition and Toxicity of Biogas Produced from Different Feedstocks in California. *Environmental Science & Technology*, *53*(19), 11569. https://doi.org/10.1021/ACS.EST.9B03003

Liu, D., Sun, Y., Li, Y., & Lu, Y. (2017). Perturbation of formate pathway and NADH pathway acting on the biohydrogen production. *Scientific Reports*, *7*(1). https://doi.org/10.1038/s41598-017-10191-7

Lu, C., Wang, Y., Lee, D. J., Zhang, Q., Zhang, H., Tahir, N., Jing, Y., Liu, H., & Zhang, K. (2019). Biohydrogen production in pilot-scale fermenter: Effects of hydraulic retention time and substrate concentration. *Journal of Cleaner Production*, *229*, 751–760. https://doi.org/10.1016/J.JCLEPRO.2019.04.233

Łukajtis, R., Hołowacz, I., Kucharska, K., Glinka, M., Rybarczyk, P., Przyjazny, A., & Kamiński, M. (2018). Hydrogen production from biomass using dark fermentation. In *Renewable and Sustainable Energy Reviews* (Vol. 91, pp. 665–694). Elsevier Ltd. https://doi.org/10.1016/j.rser.2018.04.043

Manigandan, S., T R, P., Anderson, A., Maryam, A. M., & Mahmoud, E. (2023). Benefits of pretreated water hyacinth for enhanced anaerobic digestion and biogas production. *International Journal of Thermofluids*, *19*. https://doi.org/10.1016/j.ijft.2023.100369

Mata-Alvarez, J. (2003). *Biomethanization of the organic fraction of municipal solid wastes*. IWA.

Mechery, J., Biji, B., Thomas, D. M., & Sylas, V. P. (2017). Biohydrogen production by locally isolated facultative bacterial species using the biomass of Eichhornia crassipes: effect of acid and alkali treatment. *Energy, Ecology and Environment*, *2*(5), 350–359. https://doi.org/10.1007/S40974-017-0069-4

Mishra, P., Krishnan, S., Rana, S., Singh, L., Sakinah, M., & Ab Wahid, Z. (2019). Outlook of fermentative hydrogen production techniques: An overview of dark, photo and integrated dark-photo fermentative approach to biomass. In *Energy Strategy Reviews* (Vol. 24, pp. 27–37). Elsevier Ltd. https://doi.org/10.1016/j.esr.2019.01.001

Nathoa, C., Sirisukpoca, U., & Pisutpaisal, N. (2014). Production of hydrogen and methane from banana peel by two phase anaerobic fermentation. *Energy Procedia*, *50*, 702–710. https://doi.org/10.1016/j.egypro.2014.06.086

Nikolaidis, P., & Poullikkas, A. (2017). A comparative overview of hydrogen production processes. *Renewable and Sustainable Energy Reviews*, *67*, 597–611. https://doi.org/10.1016/J.RSER.2016.09.044

Nugraha, W. D., Syafrudin, Pradita, L. L., Matin, H. H. A., & Budiyono. (2018). Biogas Production from Water Hyacinth (Eichhornia Crassipes): The Effect of F/M Ratio. *IOP Conference Series: Earth and Environmental Science*, *150*(1). https://doi.org/10.1088/1755-1315/150/1/012019

Odedina, M. J., Charnnok, B., Saritpongteeraka, K., & Chaiprapat, S. (2017). Effects of size and thermophilic pre-hydrolysis of banana peel during anaerobic digestion, and biomethanation potential of key tropical fruit wastes. *Waste Management*, *68*, 128–138. https://doi.org/10.1016/J.WASMAN.2017.07.003

Ohnishi, A., Hasegawa, Y., Fujimoto, N., & Suzuki, M. (2022). Biohydrogen production by mixed culture of Megasphaera elsdenii with lactic acid bacteria as Lactate-driven dark fermentation. *Bioresource Technology*, *343*, 126076. https://doi.org/10.1016/J.BIORTECH.2021.126076

Omondi, E. A., Ndiba, P. K., & Njuru, P. G. (2019). Characterization of water hyacinth (E. crassipes) from Lake Victoria and ruminal slaughterhouse waste as co-substrates in biogas production. *SN Applied Sciences*, *1*(8). https://doi.org/10.1007/s42452-019-0871-z

Osman, A. I., Deka, T. J., Baruah, D. C., & Rooney, D. W. (2020). Critical challenges in biohydrogen production processes from the organic feedstocks. In *Biomass Conversion and Biorefinery*. Springer. https://doi.org/10.1007/s13399-020-00965-x

Osman, A. I., Skillen, N. C., Robertson, P. K. J., Rooney, D. W., & Morgan, K. (2020). Exploring the photocatalytic hydrogen production potential of titania doped with alumina derived from foil waste. *International Journal of Hydrogen Energy*, *45*(59), 34494–34502. https://doi.org/10.1016/j.ijhydene.2020.02.065

Parra, D., Valverde, L., Pino, F. J., & Patel, M. K. (2019). A review on the role, cost and value of hydrogen energy systems for deep decarbonisation. *Renewable and Sustainable Energy Reviews*, *101*, 279–294. https://doi.org/10.1016/J.RSER.2018.11.010

Pérez-Rangel, M., Barboza-Corona, J. E., Buitrón, G., & Valdez-Vazquez, I. (2020). Essential Nutrients for Improving the Direct Processing of Raw Lignocellulosic Substrates Through the Dark Fermentation Process. *Bioenergy Research*, *13*(1), 349–357. https://doi.org/10.1007/S12155-019-10083-W/TABLES/5

Policastro, G., Carraturo, F., Compagnone, M., Guida, M., & Fabbricino, M. (2022). Enhancing hydrogen production from winery wastewater through fermentative microbial culture selection. *Bioresource Technology Reports*, *19*, 101196. https://doi.org/10.1016/J.BITEB.2022.101196

Policastro, G., Lamboglia, R., Fabbricino, M., & Pirozzi, F. (2022). Enhancing Dark Fermentative Hydrogen Production from Problematic Substrates via the Co-Fermentation Strategy. *Fermentation*, *8*(12). https://doi.org/10.3390/fermentation8120706

Qu, X., Zeng, H., Gao, Y., Mo, T., & Li, Y. (2022). *Bio-hydrogen production by dark anaerobic fermentation of organic wastewater*. https://doi.org/10.3389/fchem.2022.978907

Rafieenia, R., Lavagnolo, M. C., & Pivato, A. (2018). Pre-treatment technologies for dark fermentative hydrogen production : Current advances and future directions. *Waste Management*, *71*, 734–748. https://doi.org/10.1016/J.WASMAN.2017.05.024

Rajagopalan, G., He, J., & Yang, K. L. (2014). Direct fermentation of xylan by Clostridium strain BOH3 for the production of butanol and hydrogen using optimized culture medium. *Bioresource Technology*, *154*, 38–43. https://doi.org/10.1016/J.BIORTECH.2013.11.094

Randolph, K., Studer, S., Liu, H., Beliaev, A., & Holladay, J. (2017). Hydrogen production cost from fermentation. DOE Hydrogen and Fuel Cells Program Record, 16016.

Richard, E. N., Hilonga, A., Machunda, R. L., & Njau, K. N. (2019). A review on strategies to optimize metabolic stages of anaerobic digestion of municipal solid wastes towards enhanced resources recovery. In *Sustainable Environment Research* (Vol. 1, Issue 1). BioMed Central Ltd. https://doi.org/10.1186/s42834-019-0037-0

Rizwan, M., Shah, S. H., Mujtaba, G., Mahmood, Q., Rashid, N., & Shah, F. A. (2019). Ecofuel feedstocks and their prospect. *Advanced Biofuels: Applications, Technologies and Environmental Sustainability*, 3–16. https://doi.org/10.1016/B978-0-08-102791-2.00001-5

Ruan, T., Zeng, R., Yin, X. Y., Zhang, S. X., & Yang, Z. H. (2016). Water Hyacinth (Eichhornia crassipes) Biomass as a Biofuel Feedstock by Enzymatic Hydrolysis. *BioResources*, *11*(1), 2372–2380. https://doi.org/10.15376/BIORES.11.1.2372-2380

Santiago, S. G., Morgan-Sagastume, J. M., Monroy, O., & Moreno-Andrade, I. (2020). Biohydrogen production from organic solid waste in a sequencing batch reactor: An optimization of the hydraulic and solids retention time. *International Journal of Hydrogen Energy*, *45*(47), 25681–25688. https://doi.org/10.1016/J.IJHYDENE.2019.11.224

Santiago, S. G., Trably, E., Latrille, E., Buitrón, G., & Moreno-Andrade, I. (2019). The hydraulic retention time influences the abundance of Enterobacter, Clostridium and Lactobacillus

during the hydrogen production from food waste. *Letters in Applied Microbiology*, *69*(3), 138–147. https://doi.org/10.1111/lam.13191

Sarangi, P. K., & Nanda, S. (2020). Biohydrogen Production Through Dark Fermentation. *Chemical Engineering & Technology*, *43*(4), 601–612. https://doi.org/10.1002/CEAT.201900452

Sarto, S., Hildayati, R., & Syaichurrozi, I. (2019). Effect of chemical pretreatment using sulfuric acid on biogas production from water hyacinth and kinetics. *Renewable Energy*, *132*, 335–350. https://doi.org/10.1016/j.renene.2018.07.121

Sevilimedu Veeravalli, S. (2014). *Biological hydrogen production from lignocellulosic biomass in an up-flow anaerobic sludge blanket reactor using mixed microbial cultures*. https://scholar.uwindsor.ca/cgi/viewcontent.cgi?article=6087&context=etd

Sivagurunathan, P., & Lin, C. Y. (2020). Biohydrogen Production From Beverage Wastewater Using Selectively Enriched Mixed Culture. *Waste and Biomass Valorization*, *11*(3), 1049–1058. https://doi.org/10.1007/S12649-019-00606-Z/TABLES/6

Soares, J. F., Confortin, T. C., Todero, I., Mayer, F. D., & Mazutti, M. A. (2020). Dark fermentative biohydrogen production from lignocellulosic biomass: Technological challenges and future prospects. In *Renewable and Sustainable Energy Reviews* (Vol. 117). Elsevier Ltd. https://doi.org/10.1016/j.rser.2019.109484

Soeprijanto, S., Prajitno, D. H., Setiawan, B., Maghfiro, W., & Rohmawati, R. (2021). Biogas production from co-digestion of water hyacinth, banana peel and water spinach wastes using a horizontal anaerobic digester. *IOP Conference Series: Earth and Environmental Science*, *649*(1). https://doi.org/10.1088/1755-1315/649/1/012022

Soltan, M., Elsamadony, M., Mostafa, A., Awad, H., & Tawfik, A. (2019). Nutrients balance for hydrogen potential upgrading from fruit and vegetable peels via fermentation process. *Journal of Environmental Management*, *242*, 384–393. https://doi.org/10.1016/J.JENVMAN.2019.04.066

Su, H., Cheng, J., Zhou, J., Song, W., & Cen, K. (2010). Hydrogen production from water hyacinth through dark- and photo- fermentation. *International Journal of Hydrogen Energy*, *35*(17), 8929–8937. https://doi.org/10.1016/j.ijhydene.2010.06.035

Sukarni, S., Zakaria, Y., Sumarli, S., Wulandari, R., Ayu Permanasari, A., & Suhermanto, M. (2019). Physical and Chemical Properties of Water Hyacinth (Eichhornia crassipes) as a Sustainable Biofuel Feedstock. *IOP Conference Series: Materials Science and Engineering*, *515*(1). https://doi.org/10.1088/1757-899X/515/1/012070

UN Global Compact. (n.d.). Retrieved August 4, 2023, from https://unglobalcompact.org/take-action/action/carbon

U.S. Energy Information Administration. (n.d.). Retrieved August 4, 2023, from https://www.eia.gov/coal/production/quarterly/co2_article/co2.html

Vasmara, C., Pindo, M., Micheletti, D., & Marchetti, R. (2018). Initial pH influences microbial communities composition in dark fermentation of scotta permeate. *International Journal of Hydrogen Energy*, *43*(18), 8707–8717. https://doi.org/10.1016/J.IJHYDENE.2018.03.122

Wang, R., Zhao, S., Wang, Z., & Koffas, M. A. (2020). Recent advances in modular co-culture engineering for synthesis of natural products. *Current Opinion in Biotechnology*, *62*, 65–71. https://doi.org/10.1016/J.COPBIO.2019.09.004

Wang, Z., & Calderon, M. M. (2012). Environmental and economic analysis of application of water hyacinth for eutrophic water treatment coupled with biogas production. *Journal of Environmental Management*, *110*, 246–253. https://doi.org/10.1016/j.jenvman.2012.06.031

Wang, Z., Zheng, F., & Xue, S. (2019). The economic feasibility of the valorization of water hyacinth for bioethanol production. *Sustainability (Switzerland)*, *11*(3). https://doi.org/10.3390/su11030905

Wauton, & William-Ebi. (2019). Characterization Of Water Hyacinth (Eichhornia Crassipes) For The Production Of Thermochemical Fuels. In *Journal of Multidisciplinary Engineering Science Studies (JMESS)* (Vol. 5). www.jmess.org

Wazeri, A., Elsamadony, M., Roux, S. Le, Peu, P., & Tawfik, A. (2018). Potentials of using mixed culture bacteria incorporated with sodium bicarbonate for hydrogen production from water hyacinth. *Bioresource Technology*, *263*, 365–374. https://doi.org/10.1016/j.biortech.2018.05.021

Weinrich, S. 1985-, Nelles, M. 1966-, & Deutsches Biomasseforschungszentrum. (n.d.). *Basics of anaerobic digestion biochemical conversion and process modelling*.

Wong, Y. M., Wu, T. Y., & Juan, J. C. (2014). A review of sustainable hydrogen production using seed sludge via dark fermentation. *Renewable and Sustainable Energy Reviews*, *34*, 471–482. https://doi.org/10.1016/J.RSER.2014.03.008

World Nuclear Association. (n.d.). Retrieved August 4, 2023, from https://www.world-nuclear.org/information-library/facts-and-figures/heat-values-of-various-fuels.aspx

Xu, J. F., Mi, Y. T., & Ren, N. Q. (2016). Buffering action of acetate on hydrogen production by Ethanoligenens harbinense B49. *Electronic Journal of Biotechnology*, *23*, 7–11. https://doi.org/10.1016/J.EJBT.2016.07.002

Yang, G., Hu, Y., & Wang, J. (2019). Biohydrogen production from co-fermentation of fallen leaves and sewage sludge. *Bioresource Technology*, *285*. https://doi.org/10.1016/j.biortech.2019.121342

Yang, G., & Wang, J. (2019). Biohydrogen production by co-fermentation of sewage sludge and grass residue: Effect of various substrate concentrations. *Fuel*, *237*, 1203–1208. https://doi.org/10.1016/j.fuel.2018.10.026

Yi, J., Dong, B., & Dai, J. J. (2014). Effect of Increasing Total Solids Contents on Anaerobic Digestion of Food Waste under Mesophilic Conditions: Performance and Microbial Characteristics Analysis. *PLoS ONE*, *9*(7), 102548. https://doi.org/10.1371/journal.pone.0102548

Yuan, Q., Liu, S., Ma, M.-G., Ji, X.-X., Choi, S.-E., & Si, C. (n.d.). *The Kinetics Studies on Hydrolysis of Hemicellulose*. https://doi.org/10.3389/fchem.2021.781291

Zagrodnik, R., & Seifert, K. (2020). Direct fermentative hydrogen production from cellulose and starch with mesophilic bacterial consortia. *Polish Journal of Microbiology*, *69*(1), 109–120. https://doi.org/10.33073/PJM-2020-015

Zhang, G. (2021). *Scholarship at UWindsor Scholarship at UWindsor Hydrogen Production During the Dark Fermentation of Glycerol Hydrogen Production During the Dark Fermentation of Glycerol*. Electronic Theses and Dissertations. 8865. University of Windsor, Canada. https://scholar.uwindsor.ca/etd/8865

APPENDIXES

Appendix A: Pretreatment of the samples

Sun-drying

7 days sun-drying

Oven drying at 105oC for 24h

Grinding in a mortar using a pestle and bottling in air-tight plastic bottles

Appendix B: The LIBS analysis process

Drying of the sample

Scanning of the sample in the optic microscope

BP

WHL

WHS

The scanned pictures of the samples

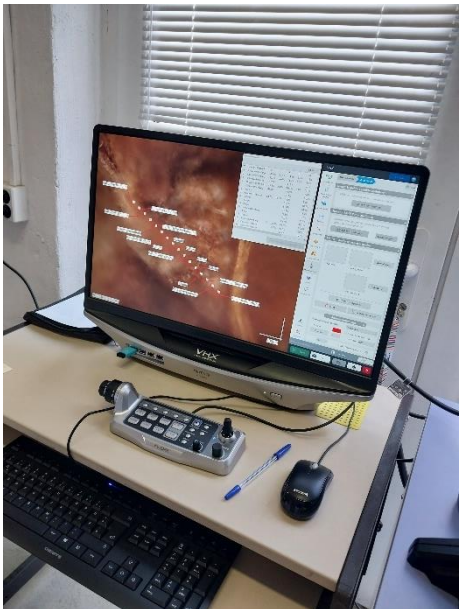

Analysis with the LIBS Analyzer

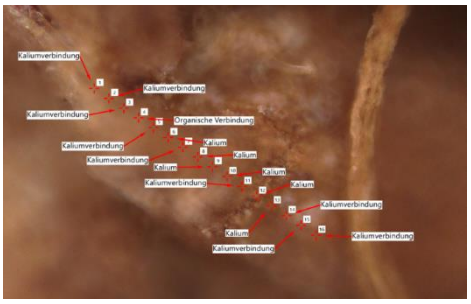

Multi-points line analysis

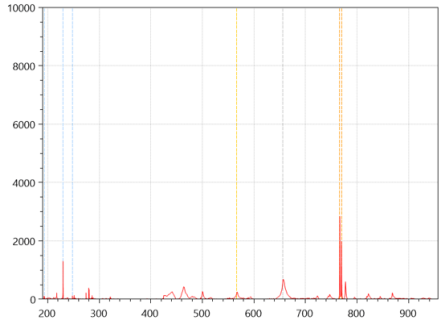

Graphs of the elements

Appendix C: Some materials used in the Fiber Analysis

The Fibretherm FT 12

Fibrebags with samples and Glass Spacers placed on a Carousel

Appendix D: Ultimate analysis data

Banana Peels					
	C	**H**	**O**	**K**	**Si**
1	46.0%	19.2%	0.0%	34.8%	0.0%
2	52.9%	11.0%	24.6%	11.5%	0.0%
3	59.5%	16.1%	0.0%	20.3%	4.1%
4	53.9%	13.0%	0.0%	30.7%	2.4%
5	32.6%	11.4%	36.5%	19.5%	0.0%
Mean	48.98%	14.14%	12.22%	23.36%	1.30%
Standard Error	4.62%	1.55%	7.72%	4.18%	0.84%

Water Hyacinth Leaves						
	C	**H**	**O**	**K**	**Na**	**Si**
1	30.30%	8.90%	44.80%	14.80%	1.20%	0.00%
2	28.10%	10.10%	55.90%	4.60%	1.30%	0.00%
3	59.70%	16.50%	0.00%	15.20%	3.10%	5.50%
4	34.80%	8.30%	48.10%	6.60%	2.20%	0.00%
5	0.00%	46.60%	0.00%	36.40%	4.80%	12.20%
Mean	30.58%	18.08%	29.76%	15.52%	2.52%	3.54%
Standard Error	9.51%	7.28%	12.28%	5.64%	0.67%	2.41%

Water Hyacinth Roots							
	C	**H**	**O**	**K**	**Na**	**Ca**	**Si**
1	21.80%	9.70%	47.90%	14.40%	6.20%	0.00%	0.00%
2	31.10%	7.90%	45.20%	10.70%	5.10%	0.00%	0.00%
3	0.00%	0.00%	48.10%	43.20%	4.60%	2.20%	1.90%
4	12.70%	0.00%	54.70%	24.60%	5.30%	1.60%	1.10%
5	26.60%	6.90%	42.20%	18.70%	5.60%	0.00%	0.00%
Mean	18.44%	4.90%	47.62%	22.32%	5.36%	0.76%	0.60%
Standard Error	5.53%	2.05%	2.07%	5.71%	0.27%	0.47%	0.39%

Water hyacinth Stems					
	C	**H**	**O**	**K**	**Na**
1	23.20%	8.30%	52.00%	12.30%	4.20%
2	29.00%	9.50%	47.20%	11.10%	3.20%
3	25.30%	9.00%	51.50%	8.40%	5.80%
4	30.20%	9.90%	47.40%	9.20%	3.30%
5	35.80%	7.30%	41.40%	12.70%	3.00%
Mean	28.70%	8.80%	47.90%	10.74%	3.90%
Standard Error	2.17%	0.46%	1.91%	0.84%	0.52%

Appendix E: Proximate analysis data

Water hyacinth distribution		
	mass	**proportion**
sample	114.50	100%
leaves	20.80	18.17%
stems	76.70	66.99%
roots	17.50	15.28%

Proximate analysis data of the samples						
	Parameters	1	2	3	Mean	Standard Error
Banana Peels	Empty mass, dry crucible (g)	65.1263	67	55.453		
	Total mass: Crucible +sample (g)	74.9282	82.673	70.8173		
	Total mass after drying 105ºC (g)	74.6472	82.2042	70.3669		
	Total mass after incineration 550ºC	66.7543	69.5566	57.971		
	Initial mass (Mi)	9.8019	15.673	15.3643		
	Dried Mass (Md)	9.5209	15.2042	14.9139		
	Mass ash (Mash)	1.628	2.5566	2.518		
	Ash Content (AC)	16.6090	16.3121	16.3886	**16.4366**	**0.0890**
	Volatile Solid (VS)	80.5242	80.6967	80.6799	**80.6336**	**0.0549**
	Total Solid (TS)	97.1332	97.0089	97.0685	**97.0702**	**0.0359**
	MC (wet basis)	2.8668	2.9911	2.9315	**2.9298**	**0.0359**
Water Hyacinth Leaves	Empty mass, dry crucible g	61.621	76.3937	61.0827		
	Total mass: Crucible +sample g	66.6942	80.0293	65.4815		
	Total mass after drying 105ºC g	66.3648	79.7944	65.1937		
	Total mass after incineration 550ºC	62.4039	76.966	61.7824		
	Mi	5.0732	3.6356	4.3988		
	Md	4.7438	3.4007	4.111		
	Mash	0.7829	0.5723	0.6997		
	AC	15.4321	15.7416	15.9066	**15.6934**	**0.1391**
	VS	78.0750	77.7973	77.5507	**77.8077**	**0.1514**
	TS (wet basis)	93.5071	93.5389	93.4573	**93.5011**	**0.0237**
	MC (wet basis)	6.4929	6.4611	6.5427	**6.4989**	**0.0237**
Water Hyacinth Stems	Empty mass, dry crucible g	59.9578	69.3798	63.1817		
	Total mass: Crucible +sample g	64.1612	73.0259	66.2112		
	Total mass after drying 105ºC g	63.9062	72.7832	66.0087		
	Total mass after incineration 550ºC	60.9257	70.2213	63.8852		
	Mi	4.2034	3.6461	3.0295		
	Md	3.9484	3.4034	2.827		
	Mash	0.9679	0.8415	0.7035		
	AC	23.0266	23.0795	23.2217	**23.1092**	**0.0582**
	VS	70.9069	70.2641	70.0941	**70.4217**	**0.2475**
	TS (wet basis)	93.9335	93.3436	93.3157	**93.5309**	**0.2014**
	MC (wet basis)	6.0665	6.6564	6.6843	**6.4691**	**0.2014**
Water Hyacinth Roots	Empty mass, dry crucible g	60.9865	60.2064	60.6746		
	Total mass: Crucible +sample g	65.7452	64.5753	66.7782		
	Total mass after drying 105oC g	65.5116	64.3946	66.4808		
	Total mass after incineration 550oC	62.0986	61.2305	62.142		
	Mi	4.7587	4.3689	6.1036		
	Md	4.5251	4.1882	5.8062		
	Mash	1.1121	1.0241	1.4674		
	AC	23.3698	23.4407	24.0415	**23.6174**	**0.2131**
	VS	71.7213	72.4233	71.0859	**71.7435**	**0.3862**
	TS (wet basis)	95.0911	95.8639	95.1275	**95.3608**	**0.2518**
	MC (wet basis)	4.9089	4.1360	4.8725	**4.6392**	**0.2518**

Appendix F : Fiber content analysis data

Samples	TS (%wt)	VS (wt%)	AC (wt%)	NDF	ADF	ADL
Banana Peels	97.1	80.6	16.4	43.11	32.74	21.03
Water Hyacinth Stems	93.5	70.4	23.1	49.95	31.55	4.47
Water Hyacinth Leaves	93.5	77.8	15.7	49.54	23.81	5.08
Water Hyacinth Roots	95.4	71.7	23.6	44.60	26.99	5.77

Appendix G: Economic analysis report from SPD

Economic Evaluation Report

for WH=BP, THESIS Absorption

August 4, 2023

1. EXECUTIVE SUMMARY (2023 prices)

Total Capital Investment	10,044,000 $
Capital Investment Charged to This Project	10,044,000 $
Operating Cost	1,949,000 $/yr
Main Revenue	320,000 $/yr
Other Revenues	1,798,792 $/yr
Total Revenues	2,118,000 $/yr
Batch Size	22.42 kg MP
Cost Basis Annual Rate	6,391 kg MP/yr
Unit Production Cost	305.03 $/kg MP
Net Unit Production Cost	305.03 $/kg MP
Unit Production Revenue	331.48 $/kg MP
Gross Margin	7.98 %
Return On Investment	10.30 %
Payback Time	9.71 years
IRR (After Taxes)	2.63 %
NPV (at 7.0% Interest)	- 2,353,000 $

MP = Total Flow of Stream 'Pure-H2'

3. FIXED CAPITAL ESTIMATE SUMMARY (2023 prices in $)

3A. Total Plant Direct Cost (TPDC) (physical cost)	
1. Equipment Purchase Cost	1,613,000
2. Installation	548,000
3. Process Piping	564,000
4. Instrumentation	645,000
5. Insulation	48,000
6. Electrical	161,000
7. Buildings	726,000
8. Yard Improvement	242,000
9. Auxiliary Facilities	645,000
TPDC	5,192,000
3B. Total Plant Indirect Cost (TPIC)	
10. Engineering	1,298,000
11. Construction	1,817,000
TPIC	3,115,000
3C. Total Plant Cost (TPC = TPDC+TPIC)	
TPC	8,308,000
3D. Contractor's Fee & Contingency (CFC)	
12. Contractor's Fee	415,000
13. Contingency	831,000
CFC = 12+13	1,246,000
3E. Direct Fixed Capital Cost (DFC = TPC+CFC)	
DFC	9,554,000